

Engineering antiwetting hydrophobic surfaces for membrane distillation: A review

Akbar Samadi^a, Tianlong Ni^a, Enrica Fontananova^b, Gang Tang^c, Hokyong Shon^d, Shuaifei Zhao^{a,*}

^a Deakin University, Geelong, Institute for Frontier Materials, VIC 3216, Australia

^b Institute on Membrane Technology, National Research Council of Italy ITM-CNR, Via P. Bucci CUBO 17C, 87036 Rende, CS, Italy

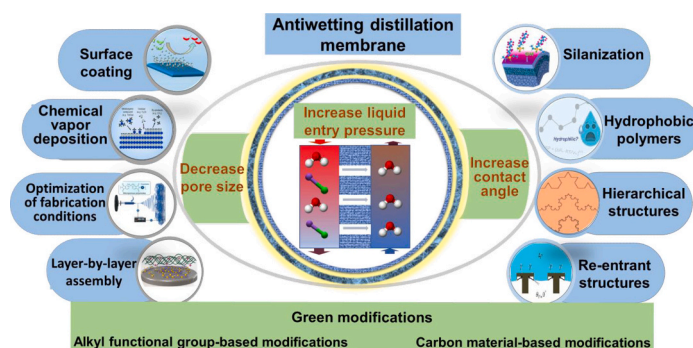
^c School of Geography, Earth and Atmospheric Sciences, The University of Melbourne, Melbourne, VIC 3010, Australia

^d School of Civil and Environmental Engineering, University of Technology Sydney, NSW 2007, Australia

HIGHLIGHTS

- We analyze the correlation between membrane properties and antiwetting performance.
- Key strategies for engineering antiwetting MD membranes are evaluated.
- Different methods and materials for antiwetting MD membranes are discussed.
- We offer insightful perspectives on engineering antiwetting MD membranes.
- This review offers comprehensive analysis and guidelines for MD membrane development.

GRAPHICAL ABSTRACT



ARTICLE INFO

Keywords:

Membrane distillation
Antiwetting
Antifouling
Liquid entry pressure
Water contact angle
Water treatment

ABSTRACT

Membrane distillation (MD) is an emerging membrane separation technology with great potential for desalination, wastewater treatment and volatile resource recovery. It becomes even more attractive as it can utilize low-grade heat or renewable energy, and treat high-salinity waste liquids towards zero liquid discharge. However, the performance of MD is often limited by the wetting of hydrophobic porous membranes during operation, leading to reduced flux and efficiency. To overcome this challenge, the development of antiwetting hydrophobic MD membranes has gained increasing attention in recent years. In this review, we examine the liquid entry pressure (LEP) and its influencing factors (e.g. the maximum pore size, surface chemistry/free energy and surface

Abbreviations: AGMD, air gap membrane distillation; APTES, 3-aminopropyl triethoxysilane; CA, contact angle; CNT, carbon nanotube; DCMD, direct contact membrane distillation; F₈, 1H, 1H, 2H, 2H-perfluorodecyl methacrylate; FAS17, 1H, 1H, 2H, 2H-perfluorodecyltrimethoxysilane; FTCS, perfluorodecyltriethoxysilane; LBL, layer-by-layer; LEP, liquid entry pressure; MD, membrane distillation; MF, microfiltration; NF, nanofiltration; PDDA, poly(diallyldimethylammonium chloride); PE, polyethylene; PES, polyethersulfone; PFOTES, poly(fluorooctyltriethoxysilane); PP, polypropylene; PPFDA, poly(1H,1H,2H,2H-perfluorodecyl acrylate); PVDF-HFP, poly(vinylidene fluoride-co-hexafluoropropylene); PDMS, polydimethylsiloxane; PTFE, polytetrafluoroethylene; PVA, poly(vinyl alcohol); PVP, poly(vinyl pyrrolidone); PVDF, polyvinylidene fluoride; RO, reverse osmosis; SEM, scanning electron microscope; SGMD, sweeping gas membrane distillation; SiA, silica aerogel; SMM, surface modifying macromolecules; VMD, vacuum membrane distillation; WCA, water contact angle.

* Corresponding author.

E-mail address: s.zhao@deakin.edu.au (S. Zhao).

<https://doi.org/10.1016/j.desal.2023.116722>

Received 17 April 2023; Received in revised form 24 May 2023; Accepted 25 May 2023

Available online 30 May 2023

0011-9164/© 2023 The Author(s). Published by Elsevier B.V. This is an open access article under the CC BY-NC-ND license (<http://creativecommons.org/licenses/by-nc-nd/4.0/>).

roughness/architecture) of an MD membrane, which determine the antiwetting performance of the porous MD membrane. From enhancing the LEP point of view, we propose two key strategies for engineering antiwetting surfaces: (1) reducing the membrane pore size, and (2) increasing the liquid contact angle by minimizing the surface free energy and the liquid/solid contact area through enhancing the surface roughness and/or creating hierarchical/re-entrant structures. These strategies include various specific fabrication techniques, such as surface coating, vapor deposition, layer-by-layer assembly, surface fluorination, and surface functionalization. Green surface modification materials and methods are also discussed to reduce the application of less environmentally friendly fluoride-containing compounds. Furthermore, we provide insights and future directions for the design and engineering of high-performance antiwetting hydrophobic MD membranes. Overall, this review offers a comprehensive analysis of the current state-of-the-art research in engineering antiwetting hydrophobic MD membranes, and highlights the potential for the development of next-generation MD membranes with improved performance and efficiency.

1. Introduction

Water scarcity is a significant global challenge that is closely linked to industrialization, urbanization, and population growth [1]. To address this problem, a variety of water/wastewater treatment technologies have been developed [2], such as adsorption [3–5], advanced oxidation [6–8], reverse osmosis (RO) [9–11], supramolecular membrane [12,13], catalysis [14–17], forward osmosis [18–20], and membrane distillation (MD) [21–23]. Although significant progress has been made with these technologies for providing clean water and resource recovery from waste, treating hypersaline wastewater (with higher salinity than typical seawater) from RO effluent and mining industries remains challenging. Among these technologies, MD has shown great promise as a solution for high-salinity wastewater treatment due to its unique driving force from the vapor partial pressure difference across the membrane [24] and its ability to be powered by low-grade heat [25], solar thermal energy [26], geothermal energy [27], or waste energy [28].

MD is a thermally-driven membrane process [29,30]. Typically, a microporous hydrophobic membrane, such as polyvinylidene fluoride (PVDF) and polytetrafluoroethylene (PTFE) membrane, acts as a barrier for the volatile vapor phase and the nonvolatile compounds of dissolved salts, whereas the water vapor passes the hydrophobic pores into the cold side [31]. The thermodynamic disequilibrium caused by the temperature difference provides a vapor partial pressure difference across the membrane, which is the driving force for water transfer (Fig. 1) [29,32,33]. Depending on the membrane pore size and mean free path of the evaporated molecules, mass transport can occur through Knudsen diffusion, molecular diffusion, and/or Poiseuille's type of flow [34,35]. Heat transport occurs through flux and conduction, leading to energy

loss in the process [36]. MD can be applied in different arrangements, including direct contact membrane distillation (DCMD), vacuum membrane distillation (VMD), air gap membrane distillation (AGMD), and sweeping gas membrane distillation (SGMD) as depicted in Fig. 2.

MD has been widely studied for desalination and wastewater treatment due to its special separation mechanism and relatively low operational requirements for pressures (1 atm) and temperatures (30–80 °C) [28]. As a result, MD membranes require less mechanical strength compared with conventional pressure-driven membrane processes, such as RO, nanofiltration (NF), and microfiltration (MF) [37]. Typical requirements of the membranes used in MD are summarized in Table 1. Theoretically, the salt rejection of MD to non-volatile compounds can be as high as 100 %. MD can produce extremely pure water for industries such as semiconductors and pharmaceuticals [38,39].

Although MD consumes more thermal energy than RO, it can still provide high water recovery at low costs if low-grade or renewable heat sources, such as solar, geothermal energy, or waste heat are available [39]. MD can also be combined with other water treatment technologies, such as electrodialysis, NF and/or RO towards zero liquid discharge [40,41]. MD is effective for waste liquids with high salinity, high oil content, and high levels of contaminants due to its insensitivity to concentration polarization and fouling under the driving force from the vapor pressure difference [1,42]. Therefore, MD has attracted growing research interests, which is reflected by the growing number of publications on “membrane distillation” (Fig. 3).

However, MD also faces several challenges, such as membrane wetting and fouling, high energy consumption, low permeation flux, and the lack of long-term stability [43–45].

Thus, MD has not been commercialized at large scales. The MD flux and thermal efficiency can be enhanced by optimizing the operating

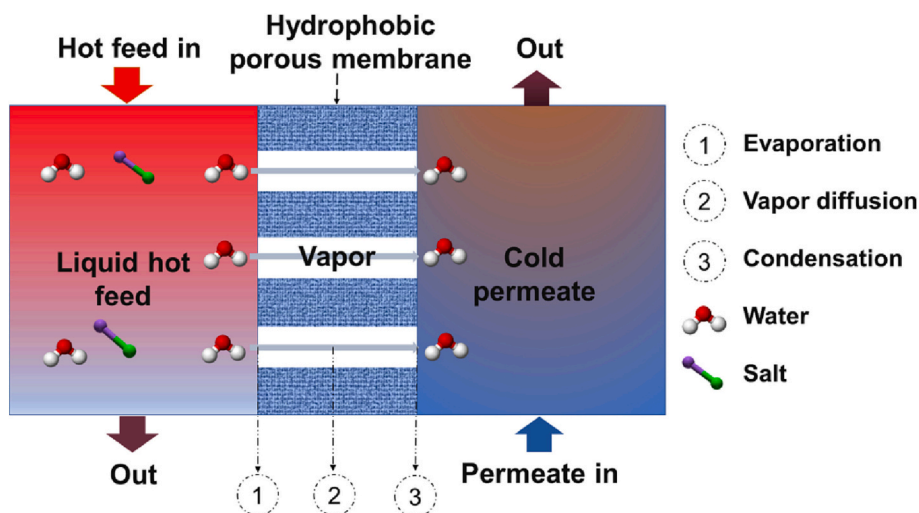


Fig. 1. Schematic illustration of a membrane distillation process.

conditions and system configuration [46]. However, wetting and fouling are the main challenges of MD as they can damage the membranes, reduce membrane permeability, and hinder their long-term operation. Fouling can have a significant impact on MD, particularly when the feed solution contains high levels of contaminants, such as dye molecules and oily substances [47–49]. These contaminants can accumulate on the membrane surface or within the pores, leading to reduced permeation flux. In addition to fouling, wetting presents a unique challenge for MD, as it can significantly increase mass transfer resistance, reduce permeation flux, and decrease energy efficiency [38]. Wetting occurs when the transmembrane pressure is higher than the liquid entry pressure (LEP) of the hydrophobic membrane, or when the membrane hydrophobicity is decreased due to the deposition/adsorption of contaminant compounds on the membrane surface or in the membrane pores [50].

Wetting can be influenced by several factors, including operational conditions, MD configurations, feed solution composition and pretreatment, membrane surface chemistry and morphology [43]. Engineering antiwetting membranes plays a vital role in addressing the challenge of wetting in MD. Therefore, there has been an increasing interest in developing antiwetting hydrophobic membranes via blending or surface engineering for MD. Blending involves incorporating hydrophobic nanomaterials or polymers to alter the internal nanostructure of the MD membrane [42]. Surface engineering for wetting resistance enhancement employs various techniques, such as surface coating, fluorination, and creating hierarchical/re-entrant structures to reduce membrane pore sizes, lower membrane surface energy, increase the surface roughness, and thus increase the water contact angle (WCA) of the membrane [51].

Table 2 provides a summary of the recent reviews on various aspects of MD membranes. However, few reviews have focused on the antiwetting engineering strategies of MD membranes, which are developed from the wetting fundamentals. Therefore, this review proposes a mathematical understanding of the wetting mechanism as a complementary approach to address the current gaps in the literature review. To gain insights into the engineering of hydrophobic antiwetting membranes for MD, an in-depth analysis of the liquid entry pressure (LEP) and its key influencing factors is provided. According to the key factors affecting the LEP, the surface modification strategies are classified into two main categories: (1) pore size reduction and (2) increasing the WCA. The conventional strategies such as surface coating or

Table 1

Typical requirements of the membranes used in MD.

Parameters	Factors affected	Typical values
Operating pressure	Wetting	~1 bar
Operating temperature	Fouling, temperature polarization, and energy efficiency	30–80 °C
Porosity	Permeability, strength, and wetting resistance	30–90 %
Water contact angle	Wetting resistance	90–160°
Liquid entry pressure	Wetting resistance	0.5–4.0 bar
Pore size	Permeability, strength, wetting resistance, and energy efficiency	0.05–0.5 μm
Thickness	Permeability, strength, wetting resistance, and energy efficiency	20–400 μm
Tortuosity	Permeability, strength, wetting resistance, and energy efficiency	1.1–3.0
Tensile strength	Strength	3.4–55.0 MPa

fluorination, and novel approaches such as the creation of hierarchical and re-entrant structures are discussed. A section is also dedicated to green surface modification methods that address the environmental issues associated with fluoride-containing compounds. Finally, the concluding remarks and future directions in this field are outlooked.

2. Wetting mechanism

The mass transfer of vapor through the MD membrane pores can be interpreted by different mechanisms based on the Knudsen number (Kn), which is the ratio between the mean free path of the vapor molecule to the characteristic length of the membrane pore channel [57]. When $Kn > 1$, the Knudsen diffusion mechanism dominates the mass transfer (Eq. (1)). When $Kn < 0.01$, continuum or ordinary molecule diffusion takes place by Eq. (2). When $0.01 < Kn < 1$, mass transfer in the transition region follows a combined Knudsen-molecular diffusion mechanism by Eq. (3) [35,58]:

$$J = \frac{2}{3} \frac{\epsilon r}{\tau \delta} \left(\frac{8M}{\pi RT} \right)^{1/2} \Delta p \quad (1)$$

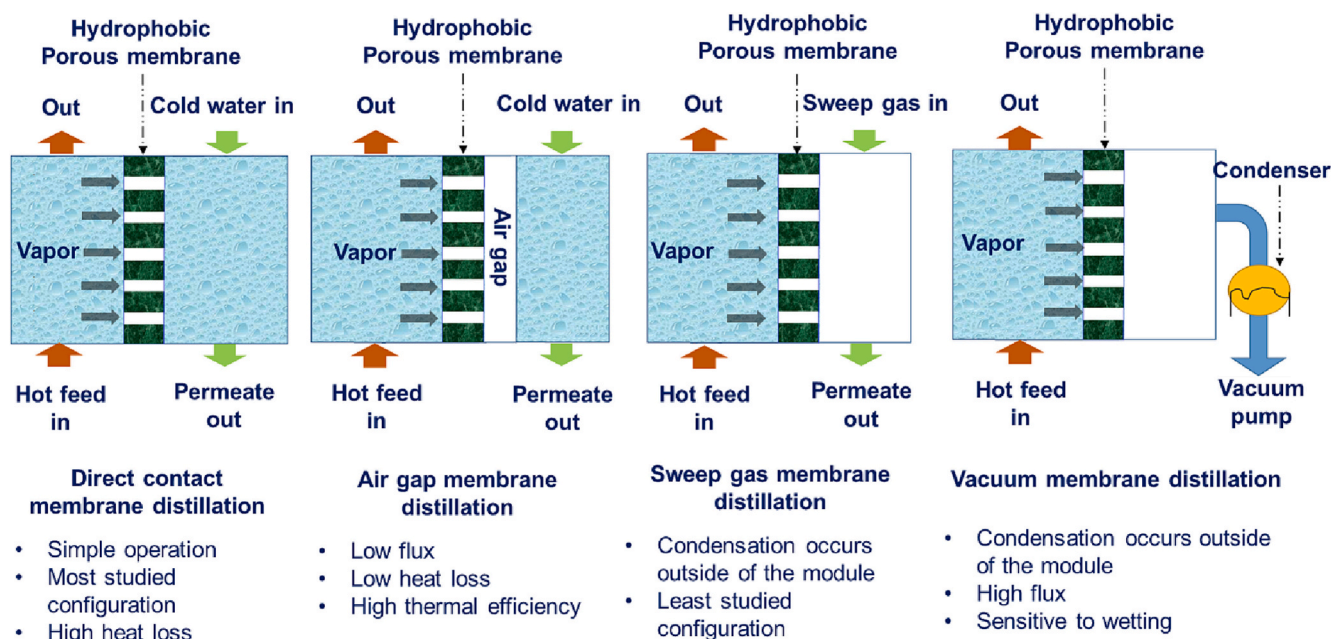


Fig. 2. Different membrane distillation configurations and their specific features.

$$J = \frac{\varepsilon}{\tau\delta} \frac{pD}{p_a} \frac{M}{RT} \Delta p \quad (2)$$

$$J = \left[\frac{3}{2} \frac{\tau\delta}{\varepsilon r} \left(\frac{\pi RT}{8M} \right)^{1/2} + \frac{\tau\delta}{\varepsilon} \frac{p_a}{pD} \frac{RT}{M} \right]^{-1} \Delta p \quad (3)$$

where D is the diffusion coefficient (m^2/s), r is pore radius (m), R is the universal gas constant ($J/Kmol$), M is molecular weight (g/mol), p_a refers to gas pressure in the pore (Pa), and p is the total pressure inside the pore ($p_a +$ vapor pressure of water). T is the absolute temperature (K), δ is the length of the vapor phase (m), ε is the membrane porosity, τ is the pore tortuosity, and Δp is the difference in vapor partial pressure through the membrane matrix (Pa).

Membrane wetting occurs when water comes into contact with air-filled pores in a hydrophobic membrane due to the balance of intermolecular force between the phases of gas, liquid, and solid [59]. Wetting involves complex physical and chemical interactions that result in the penetration of water into porous membranes [60]. In MD, the generation of a non-wetting fixed interface between the hydrophobic membrane surface and the liquid phase is the key to preventing wetting [61]. Polymeric materials, such as PVDF [62], PTFE [63], and polypropylene (PP) [64] have been widely used in MD due to their hydrophobic nature.

Fig. 4 illustrates the four states of hydrophobic membrane wetting. The transition from a non-wetting state to a surface-wetting state is driven by the push on the liquid/vapor interface towards the membrane hydrophobic channel [65]. As a result, the vapor mass transport declines gradually due to the increase in temperature polarization that declines the feed side temperature. When the feed solution enters the membrane pores, it results in partial wetting, which can decrease the permeate flux due to a decline in active air channel for mass transport (i.e. an increase in liquid phase within the channel) [50]. Finally, more and more liquid filling the membrane channel leads to complete wetting. As a result, the viscous flow of liquid water through membrane pores occurs and the MD membrane fails to operate. The wettability of an MD membrane is primarily determined by the LEP, which will be critically discussed in the next section. The membrane undergoes wetting when the transmembrane pressure (ΔP) overcomes the LEP of the membrane against a specific liquid [66].

MD is a non-isothermal process, which is influenced by the membrane microstructure, making it challenging to develop an accurate mathematical model [67]. However, a precise mathematical model is essential for in-depth analysis and optimization of the process. A study by Hitsov et al. on heat and mass transfer in MD models reveals that some physical phenomena occurring inside the membrane, such as surface diffusion, have been neglected [68]. Furthermore, the models

Table 2

Summary of the most recent reviews on the modification of hydrophobicity and anti-wetting properties of MD membrane.

Title	Review focus	Ref.
Anti-fouling and anti-wetting membranes for membrane distillation	The focus was not clear since many aspects, such as MD principles, configurations, membrane types, fabrication methods, applications and energy considerations are covered.	[1]
Non-fluoroalkyl functionalized hydrophobic surface modifications used in membrane distillation for cheaper and more environmentally friendly applications: a mini-review.	Non-fluoroalkyl materials for surface modification of MD membranes.	[52]
Membrane surface modification by electrospinning, coating, and plasma for membrane distillation applications: a state-of-the-art review	Fabrication methods: electrospinning, coating and plasma.	[53]
Pore wetting in membrane distillation: a comprehensive review.	Pore wetting parameters, causes, modelling and mitigation methods in terms of membrane fabrication, design and pretreatment.	[33]
Omniphobic membranes for distillation: opportunities and challenges	Wetting fundamentals and omniphobic membrane fabrication methods.	[46]
Biomimetic hydrophobic membrane: a review of anti-wetting properties as a potential factor in membrane development for membrane distillation (MD)	Anti-wetting factors and techniques for MD membranes.	[54]
A review of membrane wettability for the treatment of saline water deploying membrane distillation.	Wetting fundamentals, MD membrane wettability and types.	[55]
Membrane distillation: progress in the improvement of dedicated membranes for enhanced hydrophobicity and desalination performance	Methods for performance enhancement of MD membranes.	[56]

have not been fully validated by experimental data. Peña et al. introduced a mathematical model that accounts for pore wetting conditions [69]. This model investigates the effect of progressive membrane pore wetting on the decrease of permeate flux and steady-state measured pressure difference:

$$J = \text{non isothermal flux} - \text{hydraulic flux} = (1 - \alpha_i)C\Delta T_b - \alpha_i A \Delta P_i \quad (4)$$

$$J_i = \frac{E\Delta T_b A \Delta p_i^{st}}{E\Delta T_b + A \Delta p_i^{st}} \quad (5)$$

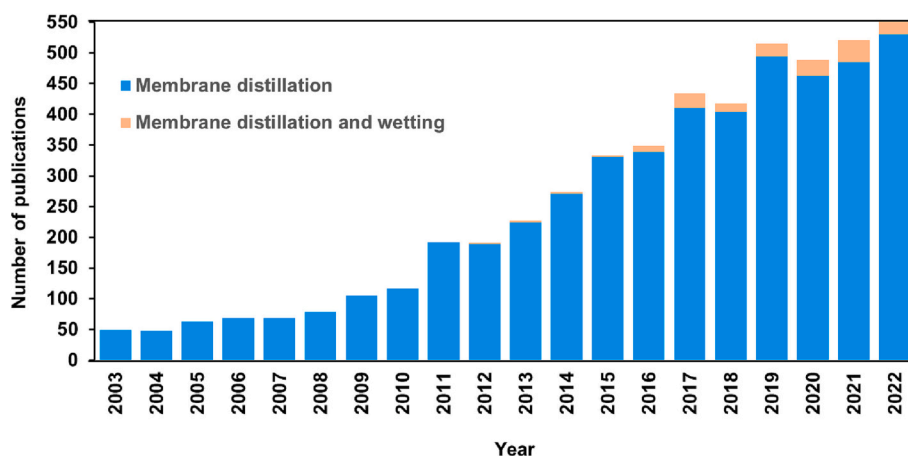


Fig. 3. The growth of research interest in membrane distillation and wetting (data from Google scholar).

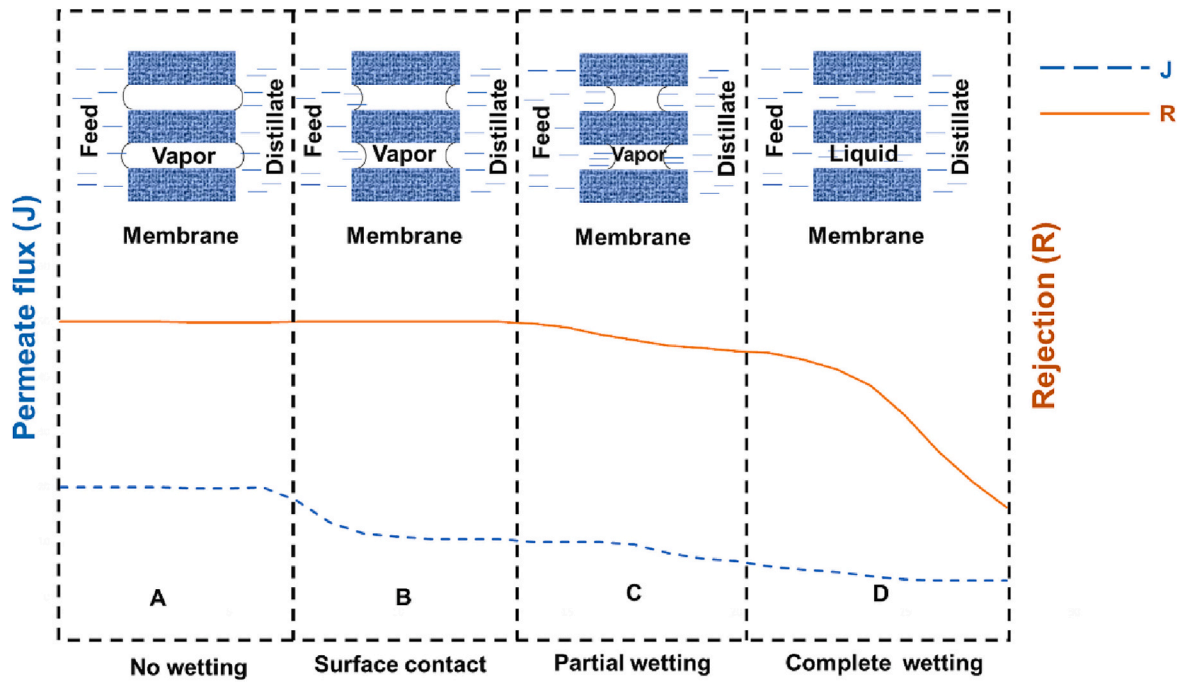


Fig. 4. Wetting evolution in the pores of a hydrophobic membrane: (A) no wetting; (B) surface wetting via contacting; (C) partial wetting; and (D) complete wetting.

$$\alpha_i = \frac{C\Delta T_b}{E\Delta T_b + A\Delta p_i^{st}} \quad (6)$$

where J_i is the volume flux (l/m^2h) at every measurement time i , C is the measured or apparent non-isothermal phenomenological coefficient, ΔT_b is the temperature difference of the bulk phases (K), A is the permeability coefficient (m^2/s), Δp_i^{st} is the steady-state measured pressure difference when the cold chamber is sealed (Pa), E is the apparent non-isothermal phenomenological coefficient, and α_i is the percentage of liquid-filled pores. This model has been used to study the wetting phenomena in MD [70].

3. Liquid entry pressure and its influencing factors

3.1. Liquid entry pressure

LEP is defined as the minimum hydrostatic pressure required to overcome the capillary pressure generated at the pores [33]. A higher LEP value indicates greater wetting resistance of the membrane against a liquid. It is suggested that a minimum LEP of 2.5 bar is required for MD [36,71], while other values have been reported for hydrophobic membranes (0.5–3.5 bar) and omniphobic membranes (1.5–5.5 bar) [46].

LEP was first defined by the Young-Laplace equation which is the classic model for the estimation of LEP in cylindrical pores [72]:

$$LEP = \frac{-2\gamma\cos\theta}{r_{max}} \quad (7)$$

where γ is the surface tension (N/m), θ is the CA ($^\circ$), and r_{max} is the maximum pore radius (m). A new term B was introduced into this equation to consider the non-cylindrical pore geometry [73]:

$$LEP = \frac{-2B\gamma\cos\theta}{r_{max}} \quad (8)$$

where B is the pore geometry coefficient. For example, the B value for stretched membranes (e.g., PTFE) with a small curvature radius is in the range of 0.4–0.6 [74]. This simple model is depicted in Fig. 5A and B. For further study of the effect of pore structure, using more realistic

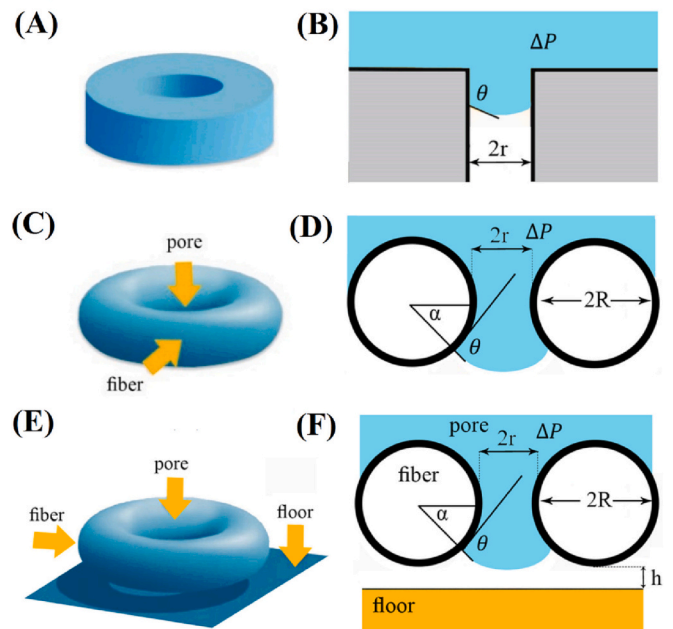


Fig. 5. (A) and (B) Cylindrical pore in the Young-Laplace model, (C) and (D) toroidal pore in the Purcell model, (E) and (F) the pore configuration for the Servi model, h is the length between the bottom of the fibers and the floor [33].

geometries, Purcell developed a model (Figs. 5C and 4D) to describe the effect of the location of the pinning point of the liquid in the pores [75]:

$$LEP = \frac{-2B\gamma\cos(\theta + \alpha)}{r(1 + R/r(1 - \cos(\alpha)))} \quad (9)$$

$$\Delta P = \frac{2\gamma}{r} \frac{\cos(\theta - \alpha)}{1 + (R/r)(1 - \cos\alpha)} = \frac{2\gamma}{r} \cos(\theta_{eff}) \quad (10)$$

where R is the fiber radius (m), α is the structural angle accounting for axial deviation of the pores ($^\circ$), and θ_{eff} is the effective CA ($^\circ$).

The Purcell model has a limitation as it predicts positive LEP values for all CA values, which contradicts the observed wetting of membranes at very low CA values [43]. The Serve model considers liquid-pore interactions below the initially wetted surface and introduced the term “floor” below each pore [76]. The LEP can be calculated by combining the two equations mentioned above into a single equation:

$$\frac{r + R(1 - \cos(\alpha))}{-\cos(\theta + \alpha)}(1 - \sin(\alpha + \theta)) = R(1 - \sin(\alpha)) + h \quad (11)$$

where h is defined as the floor height (m) describing the fibers that may attract the liquid to enter further into the membrane (Fig. 5E and F). The modified model could explain the observed LEP performance over CAs ranging from 63° to 129° [43].

By considering the effect of the axial irregularity of pores, García et al. [70] proposed the following equation for LEP based on the Peña model (Eqs. (4)–(6) [69]):

$$LEP = \frac{2\gamma}{r_{\max}} \frac{\cos(\arcsin(\varphi))}{\left[1 + \frac{2R}{r} \sin^2\left(\frac{\theta_A}{2} - \frac{\arcsin(\varphi)}{2}\right)\right]} \quad (12)$$

where r is the mean pore radius (m), θ_A is the advancing CA ($^\circ$), R is the mean curvature radius of the pore wall element (m), and $(\varphi = \frac{R \sin(\theta_A)}{1+R})$ (Fig. 6)). However, the calculation of r/R is a challenging issue when using this model.

The surface chemistry also has effects on the LEP. Therefore, García et al. proposed another equation for polar or hydrogen bonding liquids on non-polar solids, taking into account for van der Waals dispersion effects of the liquid-solid adhesion [70]:

$$LEP = \frac{2}{r_{\max}} \left(\gamma_L - 2\sqrt{\gamma_S^d \gamma_L^d} \right) = \frac{2}{r_{\max}} (\gamma_L - \gamma_L^W) \quad (13)$$

where γ_S^d and γ_L^d are the surface energies from dispersion components of

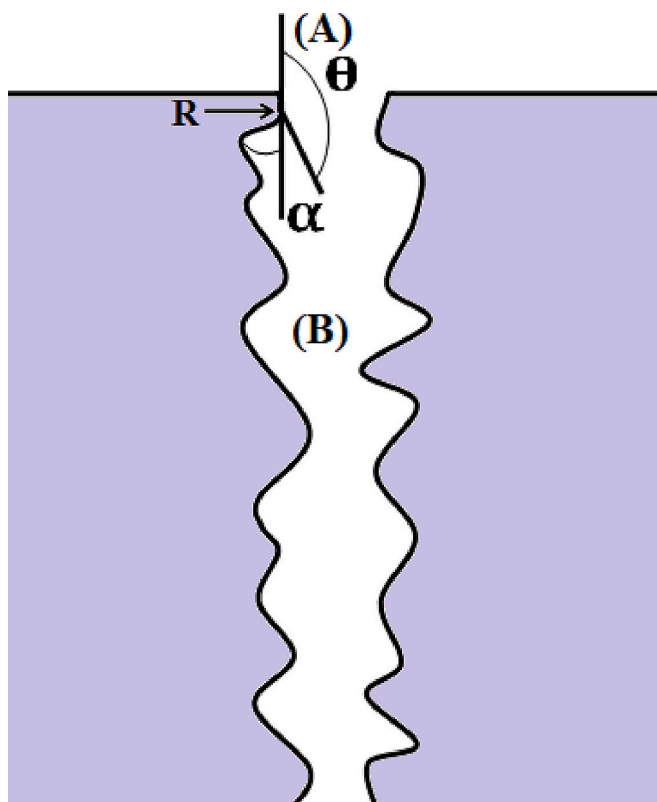


Fig. 6. Interface in the irregular pore of a hydrophobic membrane. (A) Liquid phase and (B) gas phase.

the solid and the liquid, and γ_L^W is the surface energy at wetting (i.e., $LEP = 0$). By reviewing all mentioned models for the LEP and new models based on CFD and genetic programming [77], there is a complicated relationship between the LEP and the membrane surface architecture. Apart from the operation condition and feed composition that affect membrane wetting (beyond the scope of this paper), LEP is related to several membrane parameters, such as the maximum pore size, surface chemistry, and surface architecture, which are discussed in the following section.

3.2. Membrane parameters influencing LEP

According to the equations for evaluating the LEP above, apparently the membrane pore size (particularly the maximum pore size), pore geometry and the CA of the liquid on the membrane surface are the key parameters affecting the LEP. The CA is closely related to several surface parameters, including the surface pore size, surface chemistry and surface roughness. Therefore, the membrane parameters influencing the LEP can be summarized as follows.

3.2.1. Membrane pore size

This parameter includes the maximum pore size, average pore size and pore size distribution of the membrane surface. The capillary pressure preventing the liquid from entering the pore is inversely proportional to the pore radius [33]. Typically, small pores and narrow pore size distributions are favorable to maintain a high LEP and thus high wetting resistance. However, reasonable pore sizes are more realistic since small pores will lead to low MD flux. For lab-made MD membranes, their pore sizes are often relatively large (typically $0.2\text{--}0.9\ \mu\text{m}$) to achieve high water flux [45,78,79]. For commercial hydrophobic membrane modules, their pore sizes are often very small (e.g. $0.04\ \mu\text{m}$ for the 3 M Liqui-Cell membrane module [30]) in order to achieve long-term operational stability without significant performance decline caused by membrane wetting.

3.2.2. Membrane pore geometry

Apart from the membrane pore size, the pore geometry coefficient, defined as the ratio of the membrane thickness to the equivalent pore diameter, also affects the LEP according to Eq. (8). A larger pore geometry coefficient, namely a thicker membrane with smaller pores, often suggests a higher LEP value.

3.2.3. Membrane surface chemistry (i.e., surface free energy)

Membrane surface chemistry has a significant impact on the CA, thereby affecting the LEP. A hydrophobic membrane with low surface energy often has a high CA and thus a large LEP. To enhance the anti-wetting property of the MD membrane, the membrane surface is often modified or functionalized by using materials of low surface energy, such as fluorosilanes [44,80].

3.2.4. Membrane surface roughness (i.e., architecture)

Membrane surface roughness is another important factor influencing the CA and thus the antiwetting performance of the MD membrane. Membrane surfaces often have a certain degree of roughness. The chemical heterogeneity and roughness can alter the CA, which is often evaluated by the Wenzel model [81] and the Cassie-Baxter model [82]. Higher surface roughness often results in a higher CA, a larger LEP, and thus better antiwetting performance. Single/multi-level hierarchical or re-entrant structures have been widely constructed on the membrane surfaces to enhance the CA and thus wetting resistance [79,83–85].

3.2.5. Membrane porosity and tortuosity

These two membrane parameters are also expected to affect the antiwetting performance of the membrane, although they are not considered in the equations for LEP evaluation. Lower membrane

porosity is often associated with smaller pore sizes and higher LEPs. Tortuosity is a measure of the path length and complexity of the flow channels in the membrane, and it is defined as the ratio of the actual path length of a fluid molecule to the straight-line distance between the two points. Higher tortuosity is often associated with lower porosity and higher antiwetting performance of a porous membrane.

It is worth noting that apart from these membrane parameters, surface tension of the liquid also affects the CA and thus the LEP. A liquid (e.g., oil) with lower surface tension is easier to cause wetting due to its lower CA on the membrane surface and lower LEP compared with a liquid (e.g., water) with higher surface tension.

4. Antiwetting fabrication strategies

According to the equations for evaluating the LEP in Section 3, decreasing the membrane pore size and/or increasing the CA value are the two main strategies for engineering antiwetting membranes. Typical strategies for increasing the CA include lowering the surface free energy by altering the membrane surface chemistry, and increasing the surface roughness by creating hierarchical or re-entrant structures. These approaches often also decrease the membrane pore size, thereby further enhancing the antiwetting performance of the MD membrane.

4.1. Reducing membrane pore size

The geometry parameters of membrane pores (e.g., pore size, pore size distribution, tortuosity, and pore length) are crucial in membrane performance [86–88]. According to the classic Young-Laplace equation (Eq. (7)), smaller pore sizes often result in lower porosity and higher LEPs, making the membrane more wetting resistant. However, smaller pore sizes may significantly reduce the membrane permeability [33]. Conversely, larger pore sizes and higher porosity offer higher MD flux and lower heat loss due to the lower thermal conductivity of the trapped air compared with the membrane [36], but increase the wetting risks. Therefore, the geometry parameters of membrane pores should be optimized to balance the wetting, flux, mechanical strength, and heat loss in practical applications.

4.1.1. Theory

Various mass transfer mechanisms may occur simultaneously since membranes contain pores of different sizes, as indicated by the pore size distribution [40]. In MD, the vapor transfer is determined by the mean pore size [40,56], while the LEP is inversely proportional to the maximum pore radius (Eq. (7)). Therefore, achieving maximum vapor flux requires the mean pore size to be close to the maximum pore size while maintaining the same antiwetting capability. Narrowing the membrane pore size distribution can reduce the wetting risk while maintaining the permeate flux [89], namely, narrow pore size distributions are desirable for MD membranes to provide maximum wetting resistance and maintain the permeate flux [36,77].

4.1.2. Surface modification

Surface modification has been widely used to enhance the antiwetting property of MD membranes. It often reduces the membrane pore size, resulting in higher LEP and lower flux [55]. Typical surface modification methods include surface coating [90], chemical vapor deposition (CVD) [91], plasma treatment [92], and layer-by-layer (LBL) assembly [93], mostly followed by a fluorination step to further enhance the membrane hydrophobicity [32,51,56].

4.1.2.1. Surface coating. Surface coating is a simple method to modify the hydrophobicity and wetting properties of MD membranes. Inorganic nanoparticles and hydrophobic polymers (e.g., perfluoro polymers) have been frequently coated onto the surfaces of MD membranes. As a result, the modified membrane often has reduced pore sizes, increased

surface roughness, and enhanced surface hydrophobicity after surface coating.

Inorganic nanoparticles, such as TiO_2 and SiO_2 have been widely used as a coating layer to increase the membrane hydrophobicity and wetting resistance [32,94–97]. For example, Guo et al. dispersed TiO_2 nanoparticles in silane and coated them onto an electrospun membrane by electrospraying [95]. The synergistic effect of TiO_2 and fluorine coating enabled a superhydrophobic membrane surface with a WCA up to 157° , and excellent regenerability. Wang et al. modified SiO_2 nanoparticles with chitosan and perfluorooctanoic acid, and then constructed a hydrophobic antiwetting and antifouling layer of SiO_2 , chitosan and perfluorooctanoic acid onto a PVDF substrate by spray coating [97].

In these surface coatings, the inorganic nanoparticles may have multiple roles, such as (1) providing anchoring sites for silanization and fluorination [45], (2) increasing the surface roughness of the membrane [98], and (3) enhancing the membrane robustness by constructing a relatively dense nanoparticle layer [99]. As a result, the modified membrane often exhibits reduced pore sizes and narrowed pore size distributions, leading to enhanced wetting resistance compared with the unmodified membrane.

Surface coating or modification is an essential step for nanofibrous MD membranes due to the relatively large pores of the electrospun membranes. Francis and Hilal employed electrospraying to coat a carbon nanotube (CNT) layer onto an electrospun PVDF-co-HFP membrane and enabled the modified membrane for MD applications by increasing the LEP of the membrane [100]. They also used the same coating method and material to modify a commercial PTFE membrane and achieved a robust MD membrane with enhanced antiwetting and antifouling properties [101].

However, there are still challenges with the coating of nanomaterials on the MD membrane surfaces. First, effective coating should provide high functionality, uniform dispersion, and enable strong interactions between the nanomaterials and the membrane surface [102]. Therefore, desirable nanomaterials for surface coating should have sufficient functional groups and smaller sizes for better dispersion. Otherwise, leaching of the nanomaterials may cause secondary contamination, or the coated layer may peel off during long-term operation. Unfortunately, these potential risks have not been well documented, which require further investigations in the future. Another challenge is the coating cost, including the cost of the nanomaterials and other chemicals involved. It is necessary to conduct a cost analysis before large-scale production of MD membranes by coating nanomaterials.

Hydrophobic polymers, such as polydimethylsiloxane (PDMS), Hyflon AD, and perfluorooctyltrimethoxysilane (PFTMS) have been investigated for engineering hydrophobic surfaces [78,80,103]. For instance, different amorphous perfluoro polymers of Hyflon AD were coated onto PVDF and polyethersulfone (PES) membranes by dip-coating [44,80]. The fabricated membranes showed enhanced LEPs due to the pore size reduction and surface energy reduction induced by Hyflon AD. The viscosity and concentration of the Hyflon AD had significant impacts on the membrane pore size reduction. A higher viscosity and/or a higher concentration of the hydrophobic polymer are typically more effective in decreasing the pore size, and thus increasing the LEP and mechanical strength of the membranes (Fig. 7) [44]. Reduction of the membrane pore size is also expected to increase the antifouling performance of the MD membrane.

4.1.2.2. Chemical vapor deposition. CVD is a common bottom-up modification method for creating a thin film or coating on a substrate through a chemical reaction in a gas phase. In CVD, the coating layer on the membrane surface can be well controlled by adjusting the deposition conditions, such as the deposition time, pressure and temperature [105]. Hydrophobic polymers, such as PTFE [106], poly(1H,1H,2H,2H-perfluorodecyl acrylate) (PPFDA) [91], and poly (divinylbenzene) [76] have been investigated to fabricate MD membranes with high

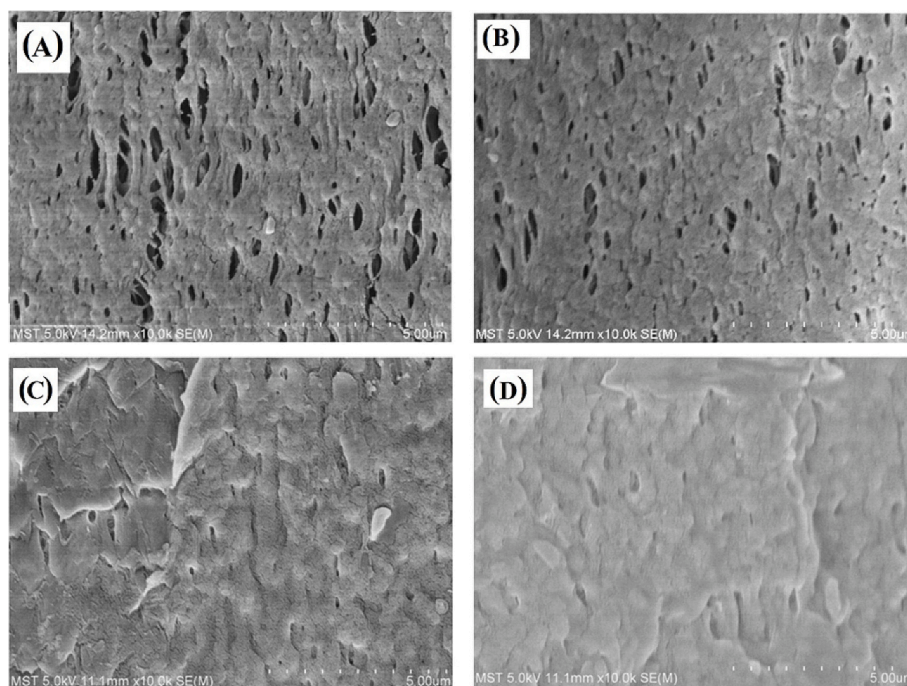


Fig. 7. Cross-section SEM images of different membranes: (A) PVDF hollow fiber, (B) PVDF hollow fiber after coating with low-viscosity Hyflon AD (0.1 wt%) [44], (C) PVDF hollow fiber after coating with high-viscosity Hyflon AD (0.5 wt%), and (D) PVDF hollow fiber after coating with high-viscosity Hyflon AD (1 wt%) [104].

wetting resistance via CVD. For example, Guo et al. deposited a thin layer of PPFDA onto an electrospun membrane via initiated CVD and reported a significant increase of the LEP from 15 to 373 kPa due to the pore size reduction of the modified membrane [91]. As a vapor-phase modification method, CVD has the advantages of precise control of the coating layer thickness and composition, using less solvents/chemicals, and avoidance of solvent-induced swelling [105]. However, CVD may face the issues of high requirements for advanced equipment (e.g., the high vacuum chamber), high complexity, high cost and low scalability.

4.1.2.3. Plasma treatment. Plasma treatment is another common surface modification technique for engineering hydrophobic MD membranes. Plasma irradiation first activates the functional groups of the membrane surface, and then the activated functional groups react with other gas or vapor in a chamber. This process is often called plasma polymerization. Fluorocarbon gas or vapor has been widely employed to deposit a thin film of CF_x by plasma polymerization to increase the hydrophobicity and thus wetting resistance of MD membranes [107]. CF₄ gas has been frequently used for surface fluorination of MD membranes by plasma polymerization [92,108]. Plasma polymerization and CVD share some technical similarities (e.g. bottom-up deposition in gas or vapor phase), and they can be used in a combination way, called plasma-enhanced CVD [105,109]. Therefore, these two surface engineering techniques also share similar advantages (e.g., using less solvent, and little swelling) and disadvantages (e.g., complex equipment requirements, high cost and low scalability). Compared with CVD, it is more difficult to precisely tailor the coating layer thickness and surface properties by plasma treatment because of the thinner layer and more adjustable parameters of the latter technique. In addition, plasma treatment may damage or significantly change the substrate polymer, complexing the surface properties of the modified membrane. The coated thin layer by plasma treatment and CVD may not be stable enough in long-term operations, which needs more investigations in the future.

4.1.2.4. Layer-by-layer assembly. LBL assembly is a fabrication technique that involves the sequential deposition of layers of oppositely

charged materials (e.g. polymers or nanoparticles) onto a substrate surface via electrostatic interaction [110–112]. Woo et al. coated multiple layers consisting of poly(diallyldimethylammonium chloride) (PDDA), silica aerogel (SiA), and 1H, 1H, 2H, 2H-

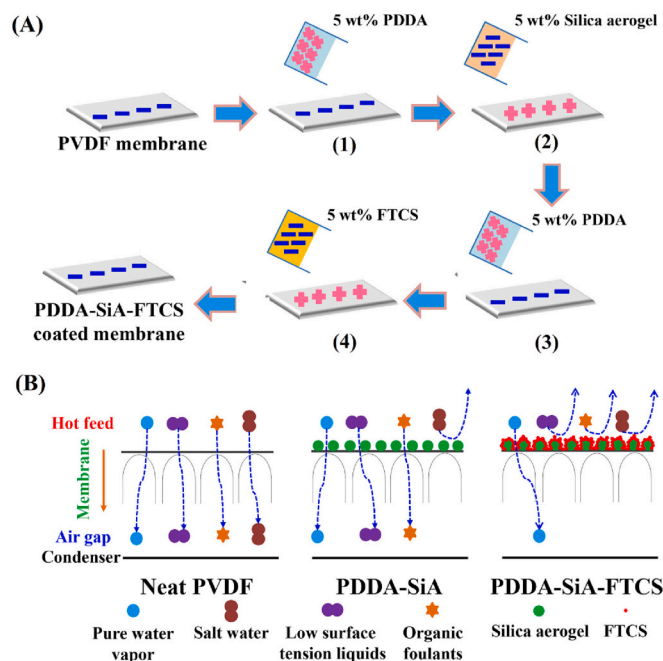


Fig. 8. (A) Layer-by-layer fabrication of a PVDF membrane to create a PDDA-SiA-FTCS multi-layer via electrostatic interaction: (1) 5 wt% PDDA solution was poured onto the neat PVDF membrane, (2) coating PDDA with 5 wt% negatively-charged silica aerogel (SiA), (3) further coating with 5 wt% PDDA and (4) final deposition of 5 wt% FTCS onto the PDDA-SiA-PDDA coated surface. (B) Antiwetting and antifouling performance illustration and comparison of the neat PVDF membrane, PDDA-SiA, and PDDA-SiA-FTCS assembled membranes in AGMD [93].

perfluorododecyltrichlorosilane (FTCS) on a PVDF membrane by LBL assembly (Fig. 8A) [93]. The pore size of the PDDA-SiA-FTCS assembled membrane reduced from 0.2 to 0.09 μm , leading to a significant rise in LEP from 0.17 to 2.04 bar. The increased surface roughness and the lowered surface energy resulted in a high WCA of 177° and a high oil CA of 163°. As a result, the PDDA-SiA-FTCS assembled membrane showed significantly enhanced antiwetting and antiwetting performance as illustrated in Fig. 8B.

LBL assembly has the advantages of precise control of the coating layer thickness, composition and surface properties as well as good scalability. However, the whole procedure may be complex and time-consuming, and require the use of toxic chemicals and charged hydrophobic polymers. These issues limit its application for engineering hydrophobic MD membranes. In addition, the assembled multiple layers may have low stabilities in long-term MD operation due to the relatively weak electrostatic adsorption force. Further chemical bonding or modification (e.g., surface fluorination) would overcome this issue. Overall, LBL assembly has not been widely used for engineering antiwetting hydrophobic MD membranes, although it has been frequently studied in fabricating antifouling hydrophilic membranes [113].

4.1.3. Improvement of synthesis method

Phase separation and electrospinning have been widely used for the preparation of MD membranes. Generally, the electrospinning method produces membranes with larger pore sizes compared with phase inversion [46]. Moreover, the electrospun membranes exhibit high WCAs due to the highly rough surfaces generated by electrospinning [53]. Phase separation is preferred when small pore sizes are required [55]. Moreover, the selection of the polymer material and the operational parameters of the phase inversion process can be easily tailored to reduce the pore sizes [32,94].

The polymer concentration of the dope solution has a significant effect on the morphology of the membrane [114]. A higher polymer concentration increases the membrane thickness and surface roughness as well as the WCA. A high polymer solution viscosity prevents the penetration of non-solvent through membrane pores, leading to a decrease in both pore size and porosity of the membrane [115]. For example, the average pore size of the PES membranes was effectively decreased by increasing the concentration of PES in the spinning dope solution [116].

Tailoring the membrane synthesis conditions has been used to reduce the membrane pore size [117]. PVDF membranes fabricated by phase inversion without any pore-forming additives exhibited small pore sizes and narrow pore size distributions [118]. Deshmukh and Li optimized the hydrophobicity, porosity, pore size distribution, and mechanical strength of a hollow fiber PVDF membrane by delaying the liquid-liquid de-mixing rate of the polymer [119]. Apart from optimizing the polymer concentration, lowering the bath temperature and increasing the thickness of the casting film can lead to denser membranes due to the reduced precipitation rate of the PVDF polymer. In summary, in membrane development by different methods (e.g., phase inversion and electrospinning) the fabrication parameters can be optimized to achieve desirable membrane pore sizes, pore size distributions, LEPs, permeate flux, and mechanical strength. For the fabrication of antiwetting MD membranes, the synthesis conditions should be optimized to achieve reasonably small pore sizes, narrow pore size distributions, and thus high LEPs for the membranes.

4.2. Increasing the contact angle

According to the equations for evaluating the LEP, increasing the liquid CA (θ) is another effective way to engineer antiwetting MD membranes. The liquid CA is affected by several membrane (e.g., surface free energy and morphology) and liquid (e.g., surface tension) properties.

4.2.1. Theory

The wettability of a solid surface with a specific liquid is commonly determined using the sessile drop method, which measures the CA of the liquid droplet on the solid surface [82]. CA is the angle of the liquid-solid interface contact with the liquid-vapor interface, reflecting the molecular interaction between solids, liquids and vapors, and the surface free energy of a solid material [55]. CA can be increased by decreasing the surface energy of the membrane via the incorporation of low surface energy materials (e.g. hydrophobic polymers) in the membrane matrix, or functionalization with low surface energy materials particularly fluorosilanes [44,80]. CA can also be enhanced by creating single-/multi-level hierarchical or re-entrant structures to minimize the fraction of the surface area that is in contact with the liquid [83,84].

The wettability of a flat and chemically homogenous surface is often evaluated by the following classic Young's eq. [120], relating the CA to the interfacial tensions of the liquid/vapor (γ_{lv}), solid/vapor (γ_{sv}) and solid/liquid (γ_{sl}) interfaces, and neglecting the surface roughness and chemical heterogeneity:

$$\cos\theta = \frac{\gamma_{sv} - \gamma_{sl}}{\gamma_{lv}} \quad (14)$$

where θ is the ideal CA. When $\gamma_{sv} > \gamma_{sl}$, then $0^\circ < \theta < 90^\circ$; when $\gamma_{sl} > \gamma_{sv}$, $90^\circ < \theta < 180^\circ$. The surface free energy of a material is the energy difference between the bulk and the surface. Calculation of the receding and advancing CAs of two different liquids on the membrane surface using the following equations give an estimation of the membrane surface energy [121].

$$\left(1 + \frac{\cos\theta_a + \cos\theta_r}{2}\right)\gamma_l = 2(\gamma_m^d \gamma_l^d)^{0.5} + (\gamma_m^{nd} \gamma_l^{nd})^{0.5} \quad (15)$$

$$\gamma_m = \gamma_m^d + \gamma_m^{nd} \quad (16)$$

where the superscripts *d* and *nd* correspond to the dispersive and nondispersive contributions to the total surface energy, respectively. Alternatively, it can be calculated using the Young equation which is related to three interfacial tensions for a droplet in contact with a solid surface [33]. The equation for the Lifshitz-van der Waals (LW) method is [122]:

$$(1 + \cos\theta)\gamma_L = 2(\gamma_S^{LW} \gamma_L^{LW})^{0.5} + 2(\gamma_S^+ \gamma_L^-)^{0.5} + 2(\gamma_S^- \gamma_L^+)^{0.5} \quad (17)$$

where *LW* (apolar), Lewis acid, and Lewis base interactions are considered to calculate the surface free energy. *S* and *L* stand for solid and liquid, respectively, while + and - are the Lewis acid and Lewis base, respectively. By using apolar liquid and/or solid, two final terms are neglected [123]. Solving this equation for three different liquids and obtaining their surface tensions from the literature and γ_L from experiments, the total surface energy of the membrane (γ_S) can be calculated by [122]:

$$\gamma_S = \gamma_S^{LW} + \gamma_S^{AB} = \gamma_S^{LW} + 2(\gamma_S^- \gamma_S^+)^{0.5} \quad (18)$$

The surface morphology is not considered in the Young's equation. Therefore, other models have been introduced to consider the effect of surface roughness and chemical heterogeneity on the CA evaluation. The WCA of a surface with chemical heterogeneity in real situations can be determined using the Wenzel model [81] and the Cassie-Baxter model [82] by Eqs. (19) and (20), respectively. The Wenzel model takes into account surface roughness and chemical homogeneity, while the Cassie-Baxter model considers chemical heterogeneity on a flat surface [32]. In the Wenzel model, liquids completely penetrate into the valleys (Fig. 9A), whereas air is trapped inside the valleys under the liquid surface in the Cassie-Baxter model (Fig. 9B) [55].

$$\cos\theta_w = r\cos\theta \quad (19)$$

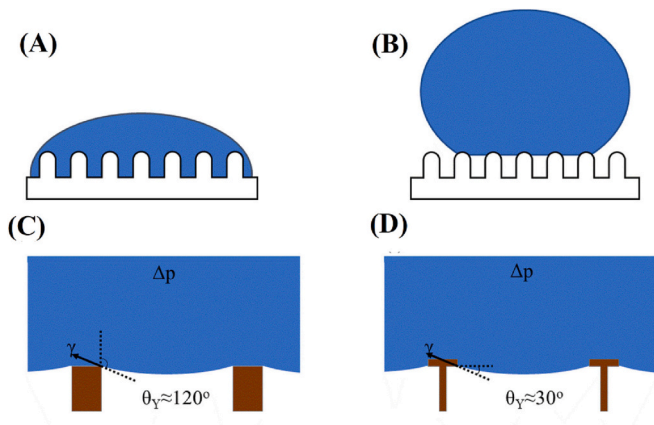


Fig. 9. (A) The Wenzel and (B) the Cassie-Baxter models of the surface wetting regime. Requirements of CA to suspend liquid: (C) simple topology; (D) reentrant topology [55].

$$\cos\theta_{CB} = f(r_f \cos\theta_Y + 1) - 1 \tag{20}$$

where θ , θ_w , and θ_{CB} are the apparent CA in the Young, Wenzel, and Cassie-Baxter models, respectively; r is the roughness factor ($r = 1$ for a smooth surface and $r > 1$ for a rough surface); r_f is the roughness ratio of wetted areas of the solid surface, and f is the fraction of the solid surface in contact with the liquid phase. When $f = 1$, then $r_f = r$ and the Cassie-Baxter equation is converted into the Wenzel equation. According to the Wenzel model, for a CA smaller than 90° , an increase in r decreases the CA. However, when a CA is larger than 90° , an increase in r amplifies the CA. The sliding angle is the minimum tilting angle required for a liquid droplet to slide down an inclined surface and has been used to determine the surface wettability. The Cassie-Baxter state provides lower sliding

angles than the Wenzel state due to the air trapped on the surface [124].

The systematic study of the hydrophobicity and membrane surface roughness is depicted in the Kao diagram (Fig. 10). In the Kao diagram, cosine values of apparent CA (θ_r) are plotted against cosine values on rigid smooth surfaces (θ_s). The Kao diagram has been used to determine when the Wenzel or Cassie-Baxter model is applicable. According to the Kao diagram, low surface free energy and high surface roughness contribute to the Cassie-Baxter state, which is desirable for superhydrophobic and omniphobic surfaces. The Wenzel state is applicable for the central region of the membrane surfaces that have homogeneous morphology with a hydrophobic surface. The first quadrant is related to the surface with high hydrophilicity. The third quadrant is the Cassie-Baxter region where high-roughness surfaces with micro-/nano-structures are developed [125].

The surface roughness represents surface irregularities and is a key factor to determine the apparent CA as illustrated by Wenzel and Cassie [126]. The roughness factor r is defined as the ratio of the actual surface area to the planar area. Atomic force microscopy has been often used to determine the roughness factors, such as the mean roughness (R_a) and the root mean square of z-direction data (R_q), according to the equations below [39]:

$$R_a = \frac{1}{L_x L_y} \int_0^{L_x} \int_0^{L_y} |f(x, y)| dx dy \tag{21}$$

$$R_q = \sqrt{\frac{\sum (Z_i - Z_m)^2}{N_p}} \tag{22}$$

where L_x and L_y are the surface dimensions in the x and y directions, and $f(x, y)$ is the surface profile related to the center plane. Z_i is the i th Z value, Z_m is the mean Z value, and N_p is the number of points for the specified area.

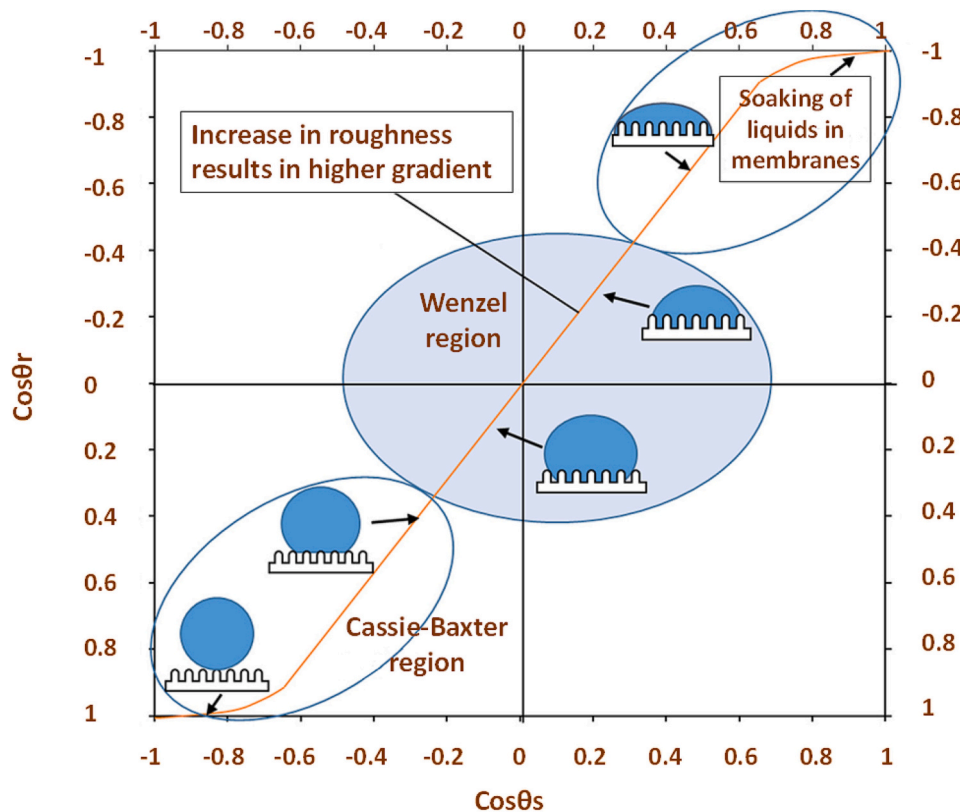


Fig. 10. The relationship between the Young's contact angle (CA) (θ_r , representing surface energy) and the apparent CA (θ_s) in terms of the surface wettability state (Wenzel/Cassie-Baxter) in Kao diagram [55].

The analysis of natural superhydrophobic surfaces, such as lotus leaves by scanning electron microscopy (SEM) revealed the multi-scale hierarchical structures (Fig. 11A) [127]. The hierarchical structures provide multi-scale surface roughness comprising nano-/micro-level structures [128]. These structures increase the fraction of the air trapped within the solid-liquid interfaces, leading to enhanced hydrophobicity and antiwetting properties [129]. The multi-scale phenomenon does not follow the classical Wenzel model and Cassie-Baxter model that are often applicable to single-scale roughness [130]. Patankar et al. [127] used a model to predict the CA of a liquid on a hierarchical structure with square pillars:

$$\cos\theta_w = \left(1 + \frac{4A_1}{(a_1/H_1)^2}\right) \cos\theta \quad (23)$$

$$\cos\theta_{CB} = \frac{1}{(b_1/a_1 + 1)^2} (\cos\theta + 1) - 1 \quad (24)$$

where H_1 is the height of the pillar, a_1 is the side length of the pillar, and b_1 is the pillar spacing. Another model for the prediction of the multi-scale surface was expressed by Mandelbrot [131]. This model introduced fractal geometry (Eqs. (25) and (26)) and could be applied to special structures as shown in the Koch curve (Fig. 11B) [132].

$$\cos\theta_w = \left(\frac{L}{l}\right)^{D-2} \cos\theta \quad (25)$$

$$\cos\theta_{CB} = f \left(\frac{L}{l}\right)^{D-2} \cos\theta - f_{LA} \quad (26)$$

where D is the Hausdorff dimension, i.e., $D = \log(4)/\log(3) = 1.2618$. L and l are the upper and lower limit scales of the fractal structure surface.

Apart from surface hierarchical structures, the re-entrant structures can gather a large number of air pockets below the liquid surface. The topology with a re-entrant structure (Fig. 9C) can exhibit high hydrophobicity even on hydrophilic materials [133]. This results in the creation of a low-energy surface with the Cassie-Baxter state, which is a physical modification of the surface [134]. Therefore, the CA can be increased by creating hierarchical re-entrant structures on the surface, even without using hydrophobic polymers for chemical modification. According to the Cassie-Baxter equation, the contribution of the surface chemistry of the material (e.g., Young's CA) to the overall hydrophobicity (e.g., apparent CA) decreases by minimizing the term f (the fraction of solid surface in contact with the liquid phase). This is depicted in Fig. 12, by plotting apparent CA versus f for different Young's CA values [83]. In this figure, for both hydrophobic and hydrophilic surfaces (with an initial CA difference of 120°), by decreasing the f value, both surfaces can become superhydrophobic; the liquid-solid contact fraction has a more pronounced effect on the apparent CA of hydrophilic surfaces.

A more hydrophobic surface with double re-entrant structures

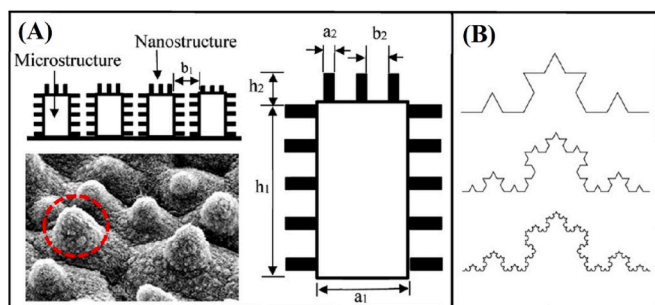


Fig. 11. (A) Model of roughness geometry for theoretical analysis; Pillars with double-scale roughness [130], and (B) Koch curve.

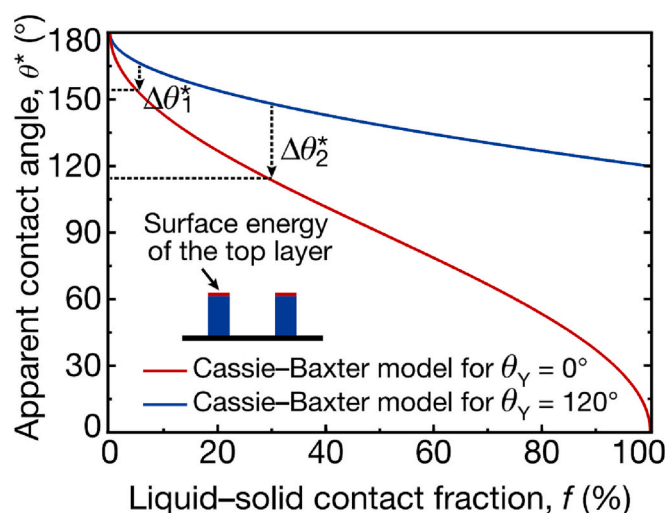


Fig. 12. Relationship between the apparent contact (θ^*) and the liquid-solid contact fraction f for an ideal Cassie-Baxter state at two different values of the Young's CA (θ_Y) [83].

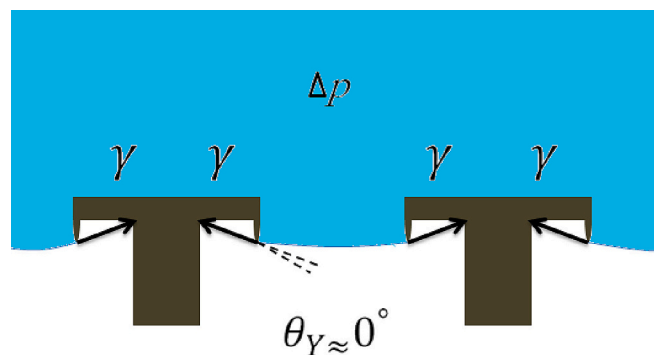


Fig. 13. Double re-entrant structure. γ is the surface tension, Δp represents the pressure difference across the membrane, and θ_Y is Young's contact angle.

(Fig. 13) has been developed and showed super-repelling for almost all liquids [135]. The structure with a top surface containing vertical overhangs at the sides stops advancing the liquid droplets that tend to wet the top surface. Double re-entrant structures provide hydrophobicity even for materials with very low Young's CA values.

According to the theoretical analysis above, we can conclude that lowering the surface free energy by engineering surface chemistry and creating special (i.e., hierarchical and/or re-entrant structures) are two effective ways to increase the CA of the membrane. Next, we will discuss them in detail.

4.2.2. Engineering surface chemistry

The membrane surface chemistry (i.e., surface free energy) is an important factor affecting the liquid-solid-gas interface, thereby determining the surface wettability. To enhance the antiwetting performance and robustness of MD membranes, incorporating hydrophobic polymers and fluorination by introducing fluorine-containing functional groups in the membrane and/or on the membrane surface have been widely studied.

4.2.2.1. Incorporating hydrophobic polymers. Hydrophobic polymers with low surface energy are often employed to engineer MD membranes for increasing their WCAs. Blending and surface modification using hydrophobic polymers are two methods to fabricate hydrophobic membranes [94,136]. The common hydrophobic functional groups include $-CH_3$, $-CH_2-CH_2-$, and $-CF_3$. The surface energy of typical

hydrophobic functional groups follows the order: CH_2 (36 dyn/cm) > CH_3 (30 dyn/cm) > CF_2 (23 dyn/cm) > CF_3 (15 dyn/cm) [137]. Accordingly, polymers such as PVDF, polytetrafluoroethylene (PTFE), polypropylene (PP), polyethylene (PE) and PDMS have low surface energy and exhibit high hydrophobicity because they do not have polar bonds to interact with the polar molecules like water [62,63,138]. Perfluorinated polymers have superior hydrophobicity and can further enhance the hydrophobicity when they are incorporated in common membranes (e.g. PVDF) [94].

PVDF was blended with PTFE particles to prepare reinforced mixed matrix membranes for MD [56]. The WCA increased from 88° for a pure PVDF membrane to 93° and 103° after incorporating 30 and 50 wt% PTFE particles, respectively. A small average pore size between 0.1 and 0.3 μm with a narrow pore size distribution exhibited enhanced water permeate flux with 40.4 $\text{L}/\text{m}^2\text{h}$ and 99.8 % salt rejection. Hydrophobic PDMS was also blended with PVDF to fabricate MD membranes, and achieved enhanced WCA from 80.2° to 111.7° [139]. The PDMS/PVDF membranes showed high average porosity and pore size at high PDMS concentrations in the polymer matrix, suggesting that low PDMS concentrations may be more desirable for enhancing the antiwetting performance of the MD membrane.

In another study, hydrophobic silicon rubber was coated onto a hydrophilic poly(phthalazine ether sulfone ketone) membrane to enhance the membrane performance [140]. The fabricated membranes showed enhanced WCA and LEP with a salt rejection of 99 %. Carbon nanotube bucky-paper membrane was coated by PTFE and exhibited superhydrophobicity with a WCA of 155° , a salt rejection of 99.9 %, and four times longer lifespan in MD operation [141]. The incorporation of PTFE as the top layer also reduced temperature polarization, which is beneficial for MD. Hydrophobic polymer coating has also been used in combination with other modifications, such as coating inorganic nanoparticles (e.g. SiO_2 and ZnO) and surface fluorination to lower the surface energy or achieve the synergistic effects from surface energy reduction and surface contact area minimization by structural engineering [142].

Recently, new hydrophobic polymers such as poly(ethene-co-chlorotrifluoroethylene) [143], poly(vinylidene fluoride-co-chlorotrifluoroethylene) [144], poly(vinylidene fluoride-co-hexafluoropropylene) (PVDF-co-HFP) [145], poly(tetrafluoroethylene-co-hexafluoropropylene) [146,147], and poly(vinylidene fluoride-cotetrafluoroethylene) [148] have been studied for the fabrication of MD membranes. They are basically fluorinated polymers that exhibit high solubility in common solvents, high hydrophobicity, and high tensile strength. However, their WCA values are still less than those of typical PTFE membranes ($>130^\circ$), and their synthesis methods are not eco-friendly and have not been fully developed [36].

Incorporating hydrophobic surface modifying macromolecules (SMM) is another method to enhance the hydrophobicity of the membrane [149,150]. Hydrophobic surface modifying macromolecules (SMM) and pore forming poly(vinyl pyrrolidone) (PVP) were used to fabricate PVDF-SMM composite membranes. Both cast and electrospun membranes exhibited higher WCAs than the PVDF membrane [149]. For the cast PVDF-SMM membrane, the LEP increased with increasing the SMM concentration due to the pore size reduction. Similar results were observed for the PVDF-SMM hollow fiber membranes [150]. In both cases, the membrane hydrophobicity was enhanced by the introduction of the hydrophobic SMM.

4.2.2.2. Fluorination. Fluorination is a common method to enhance the hydrophobicity of a membrane by introducing fluorine-containing functional groups [46]. Polymer membrane surfaces often have various functional groups, such as hydroxyl, amino, and double bonds [151–153]. The activated surfaces can react with fluoroalkyl functional groups via grafting, functionalization, polymerization, copolymerization, etc. [52]. Fluorination is often achieved in two ways. One way is to

first modify nanoparticles with fluorine-containing polymers/precursors, followed by coating, blending, or electrospinning them into or onto membranes to achieve high surface roughness and low surface energy. Another way is the direct fluorination of the membrane surface by different techniques, such as surface coating, grafting, and plasma modification using similar fluorine-containing polymers [71]. A list of common fluorination compounds is summarized in Table 3.

Inorganic nanoparticles, such as TiO_2 , ZnO, and SiO_2 have been incorporated on MD membranes to enhance their surface roughness and hierarchical/re-entrant structures [151,152]. They can be mixed in the membrane dope solution or coated onto the membrane surface [161–163]. Creating another layer on the membrane surface by fluorination of the surface nanoparticles will enable lower surface energy and hierarchical structures, resulting in more robust omniphobic or superhydrophobic membranes [52]. Most nanomaterials have hydroxyl groups that are reactive with fluoroalkylsilane compounds. A list of works on the fluorination of nanomaterial-coated MD membranes is shown in Table 4. Interestingly, the combination of nanomaterials and fluorination often leads to superhydrophobic and/or omniphobic membranes, which are highly desirable for practical MD applications due to the enhancement of the wetting resistance and robustness.

Various fluoroalkyl materials have been studied for hydrophobic modification of nanoparticle-coated MD membranes [79,173]. For example, tri-functional perfluoroalkylsilanes molecules have been used to functionalize ceramic membranes as illustrated in Fig. 14 [159]. Perfluorodecyltriethoxysilane/PDMS mixture was used for crosslinking and fluorination of 3-aminopropyl triethoxysilane (APTES)-treated PES membranes coated by silica nanoparticles [173]. The fabricated membranes exhibited anti-oil-fouling and antiwetting abilities. Amino-functionalized PVDF membranes were spray-coated by silica nanoparticles and then fluorinated by a silane solution 1H, 1H, 2H, 2H-perfluorodecyltrimethoxysilane (FAS17). The synergistic effect of silica nanoparticle deposition and fluorination increased the membrane omniphobicity with a WCA of 160° [168]. Grafting silica nanoparticles onto the membrane surface and fluorination by poly (fluorooctyltriethoxysilane) (PFOTES) enabled an omniphobic membrane with a WCA of 169° and relatively high permeate flux (37 LMH) [79].

SiO_2 is a very popular nanoparticle for the preparation of MD membranes due to its physicochemical stability, low cost, and roughness creation properties. Dong et al., fluorinated the PVDF/ SiO_2 MD membrane surface with fluoroalkylsilane and reported an increase in WCA from 130.4° to 160.5° [174]. The negative charge of the SiO_2 nanoparticles with hydroxyl groups often requires the pre-treatment of membrane surface by hydroxyl or ammonium-containing groups, such as polydopamine, trimesoyl chloride, and APTES [167]. The pre-treated PVDF membranes were coated with SiO_2 , and fluorinated with perfluoroalkylsilane, and the modified membrane exhibited a WCA higher than 150° without a significant reduction in permeate flux [167]. SiO_2 nanoparticles from tetraethyl orthosilicate precursor were deposited on cellulose nanofiber membranes by in-situ dip-coating in the presence of ammonia, and high water and oil CA values of about 150° were observed [165]. Similarly, PVDF-HFP and cetyltrimethylammonium bromide were incorporated to fabricate MD membranes. The fabricated membranes were dip-coated by SiO_2 nanoparticles and fluorinated by FAS17 via CVD, and the modified membrane showed superhydrophobicity with a WCA higher than 150° [175]. To conclude, the coupling of inorganic nanoparticle incorporation and fluorination is highly effective in creating superhydrophobic/omniphobic MD membranes with high roughness/re-entrant structures.

Fluorination can be directly performed on the membrane surface if the surface has sufficiently high roughness and reactive functional groups, such as hydroxyl, epoxide, carbonyl, and carboxylic groups, which facilitate stable fluorination. For example, GO or reduced GO has excellent chemical, mechanical, and thermal stabilities as well as high porosity and roughness [52]. Wen et al. fabricated GO and reduced GO membranes by vacuum filtration and performed fluorination with

Table 3

A list of common fluorine-containing compounds used for fluorination.

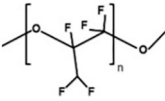
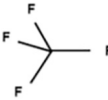
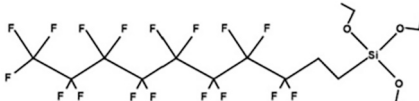
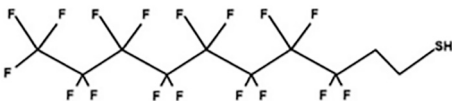
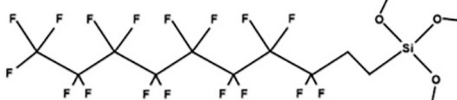
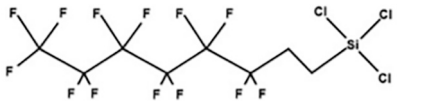
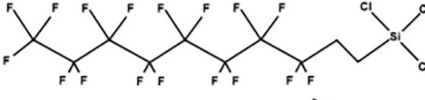

Chemical name	CAS no.	Chemical structure	Ref.
Perfluoropolyether (PFPE)	69991-67-9		[154]
Tetrafluoromethane (CF ₄)	75-73-0		[155]
1H, 1H, 2H, 2H-perfluorodecyltriethoxysilane (PFTES)	101947-16-4		[93]
1H,1H,2H,2H-perfluorodecanethiol (PFDT)	34143-74-3		[156]
1H, 1H, 2H, 2H-perfluorodecyltrimethoxysilane (FAS17)	83048-65-1		[157]
1H, 1H, 2H, 2H-perfluorooctyl-trichlorosilane (PFOTCS)	78560-45-9		[158]
1H,1H,2H,2H-perfluorodecyltrichlorosilane (FDTS)	78560-44-8		[159]
1H, 1H, 2H, 2H-perfluorooctyltriethoxysilane (PFOTES)	51851-37-7		[160]

Table 4

A selected list of works on fluorination of nanoparticle-coated MD membranes.

Polymer	Nanomaterial	Fluoroalkyl compound	Feed T (°C)	Permeate T (°C)	Feed salinity (g•L ⁻¹)	WCA (°)	Membrane flux (kg•m ⁻² •h ⁻¹)	Rejection (%)	Ref.
PVDF	CNTs	1H,1H,2H,2H-perfluorodecyltriethoxysilane	55–75	15	5	180	32.4	–	[164]
Cellulose	SiO ₂	(Heptadecafluoro-1,1,2,2-tetrahydrodecyl) trichlorosilane	60	20	58.44	151	43.6	100	[165]
PVDF-HFP	TiO ₂	1H,1H,2H,2H-perfluorooctyltriethoxysilane	60	20	35	162	38.7	–	[166]
PVDF-HFP	SiO ₂	1H,1H,2H,2H-Perfluorodecyltriethoxysilane	60	20	58.44	152	28.6	100	[167]
PVDF	SiO ₂	1H,1H,2H,2H-perfluorodecyltriethoxysilane	70	20	35	164	27.0	99.99	[168]
PDMS/PES	SiO ₂	1H,1H,2H,2H-perfluorodecyl triethoxysilane	60	20	58.44	146	29.0	99.98	[169]
PVDF	SiO ₂ /PS	1H,1H,2H,2Hperfluorodecyltrimethoxysilane	60	20	^a	176	9.0	–	[170]
PVDF	TiO ₂	(Tridecafluoro-1,1,2,2-tetrahydrooctyl) triethoxysilane	40	20	100 ^b	>150	6.0	99.9	[171]
PVDF-HFP	SiO ₂	(Heptadecafluoro-1,1,2,2-tetrahydrodecyl) trichlorosilane	60	20	58.44	150	37	100	[172]
PVDF	SiO ₂	Perfluorodecyltrichlorosilane	60	20	58.44	>150	13.6	100	[133]

^a An emulsion of sodium dodecyl sulfate: hexadecane: NaCl at a concentration ratio of 240: 2400: 10000 (mg•L⁻¹) in water was used to simulate oily waste water.

^b Gallic acid in water was used as the feed solution.

perfluoroalkylsilanes solution [176]. The fabricated membranes showed relatively high WCAs up to 144°. In another study, the WCA of organosilica membranes containing hydroxyl functional groups was improved from 50° to 105° after fluorination with PFOTES solution [177].

Membrane surface fluorination can also be achieved by plasma treatment using fluorine-containing gas, vapor or monomers. The plasma polymerization with CF₄ [155] and 1H, 1H, 2H, 2H-perfluorodecyl methacrylate (F₈) [178] has been reported to enhance membrane surface hydrophobicity. For example, PES membranes were

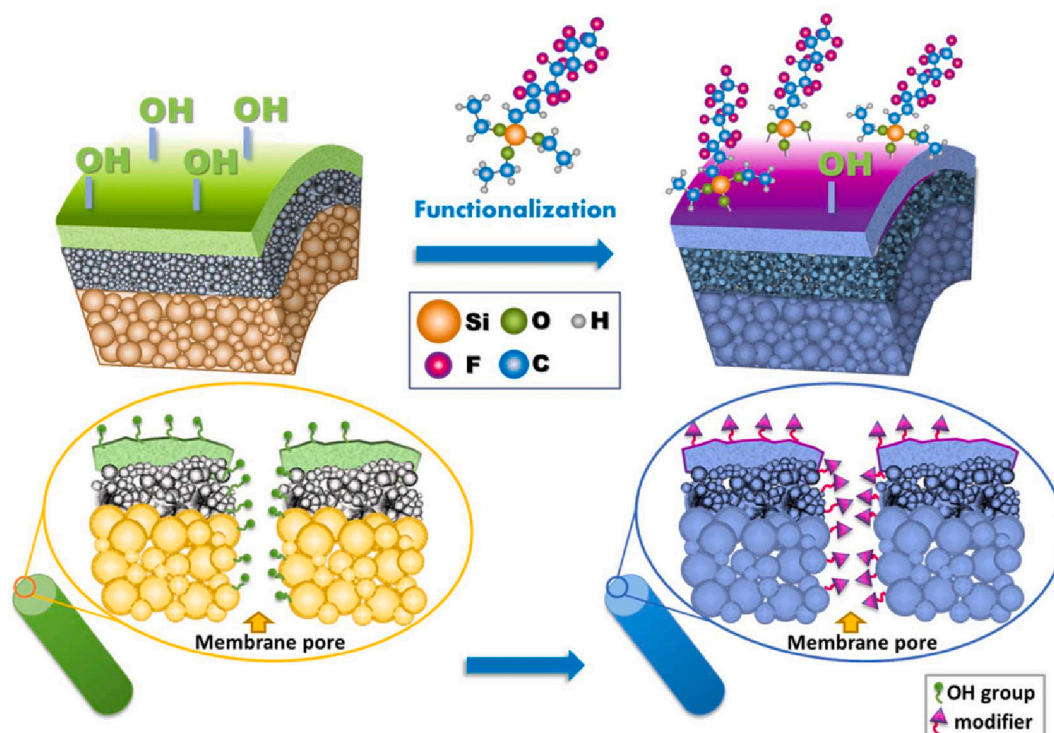


Fig. 14. Functionalization of ceramic membranes by tri-functional perfluoroalkylsilanes molecules [159].

activated by argon plasma and then fluorinated by CF_4 gas, leading to significantly improved WCAs [108]. Non-vapor F_8 monomers were applied for the plasma treatment of polyacrylonitrile membranes to enhance hydrophobicity [179]. Therefore, fluorination via plasma treatment has the potential to improve the hydrophobicity and anti-wetting performance of MD membranes. However, plasma treatment assisted surface fluorination still has some challenges as discussed in Section 4.1.2. In particular, the costs and the environmental issues of hazardous fluoroalkyl chemicals should be carefully considered in surface fluorination by plasma polymerization [180,181]. In the future, it is highly recommended to replace toxic fluorination materials with non-fluoroalkyl green agents to minimize the membrane costs and the adverse environmental impacts.

4.2.3. Engineering surface structure

Apart from engineering surface chemistry to lower the surface energy of the membrane, creating special surface structures to minimize the contact area between the liquid and the solid is another effective way to increase the CA. Hierarchical and re-entrant structures are two desirable topographical structures for roughness enhancement to engineer antiwetting superhydrophobic or omniphobic membranes for MD.

4.2.3.1. Hierarchical structure. Hierarchical structures can be prepared on the surface of composite membranes by electrospinning. This technique can produce highly porous structures, compensating for the pore size reduction. Furthermore, the addition of inorganic additives [182] to the spinning solution or coating with nanoparticles [154,183,184], followed by fluorination [154,158,184] can produce surfaces with hierarchical structures. These methods enable MD membranes with lowered surface energy and increased surface roughness, which tend to significantly increase the liquid CAs of the membranes.

Two-dimensional graphene nanoparticles were added to the PVDF dope solution to prepare electrospun membranes [185]. At the optimum graphene concentration, a very high CA of 163° and a high LEP of 187 kPa were observed due to the creation of the hierarchical structure. In another study, Sas et al. prepared electrospun fibers containing porous

micro particles [182]. The enhanced CA (162°) was reported due to the accumulation of the filler particles on the membrane surface and also nano-coating of the periphery of fibers which increases the surface roughness.

Silanization by using silane-based solutions (e.g. FTCS and APTES) is another effective way to create hierarchical structures [158,186]. For example, the dual-layer electrospinning method was applied to create fluorinated silane molecule/PVDF layers onto a glass slide, and a microscale and nanoscale hierarchical structure was observed [187]. Zheng et al. employed the synergistic effects of silica nanoparticle coating, silanization and fluorination assisted by polymer 3-methacryloxypropyltrimethoxysilane and 1H, 1H, 2H, 2H-perfluorodecyltrimethoxysilane to fabricate an omniphobic PVDF membrane with hierarchical structures with a WCA up to 176° [170].

Inorganic metalloids and metal oxides, such as SiO_2 , TiO_2 , ZnO , and Al_2O_3 have been employed to produce superhydrophobicity for MD membranes via the creation of hierarchical structures with multilevel roughness [128,188]. Particularly, TiO_2 and SiO_2 have been widely used due to their low costs, and excellent physicochemical, antifouling, and antimicrobial properties [189]. They can also be easily functionalized with fluorinated (e.g. fluoroalkylsilanes) or non-fluorinated (e.g. polyvinylsilsesquioxane) hydrophobic agents to prepare multifunctional membranes [188]. Li et al. created a pine-needle-like hierarchical nanostructure with multilevel roughness on PVDF-HFP membranes by coating fluorinated TiO_2 nanoparticles (Fig. 15) [189]. The air pockets in the nanostructures enabled a Cassie-Baxter state and fluorination provided low surface energy, leading to high CAs for water (168°) and mineral oil (153°). In another study, Razmjou et al. created hierarchical structures on PVDF membranes by coating fluorinated TiO_2 nanoparticles [128]. The fabricated membranes exhibited excellent omniphobic properties.

LbL assembly has also been used to create hierarchical structures. This process involves depositing a nano-sized roughness on a microstructure roughness [190,191]. Multi-layers of silica nanoparticles with different sizes and functionalities have been applied to create hydrophobic surfaces [191]. LBL assembly of poly(diallyldimethylammonium

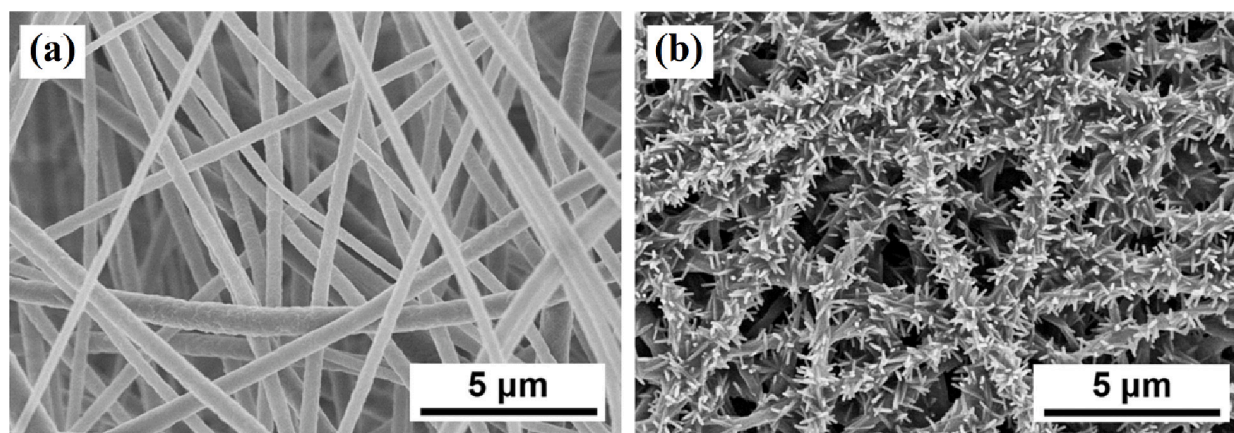


Fig. 15. SEM images of (a) pristine PVDF-HFP nanofibers and (b) fluorinated TiO_2 /PVDF-HFP nanofibers [189].

chloride), silica aerogel, and FTCS by electrostatic interaction has been used to create hierarchical structures [93]. The fabricated membranes exhibited a very high water CA of 177° and oil CA of 163° , while the permeate flux decreased due to the reduction in pore size from 0.20 to 0.09 μm . Furthermore, LBL assembly is also capable of generating Janus membranes. Deposition of catechol/chitosan and polyethyleneimine over a PVDF membrane is an example of such an approach to create hierarchical cauliflower-like morphology for the top surface [190]. The hierarchical cauliflower-like morphology of the top surface and its superhydrophilicity prevented surfactant and oil attachment via the hydration barrier effect.

4.2.3.2. Re-entrant structure. Theoretical analysis of the re-entrant structure, which is wider on top and narrower at the bottom, was introduced by Extrand [192]. He revealed that a surface with even a smooth top layer but having a re-entrant topology can have a high CA [33]. Re-entrant structures with various geometries, such as micro-mushrooms [193], micro-hoodoo arrays [84], fiber mats [194], micro-nail forests [195], micro-posts [196], and nanoparticle coatings [197] can be generated by either top-down techniques (e.g., templating) or bottom-up techniques (e.g., CVD) [55]. Tuteja et al. fabricated re-entrant structures by the lithographic method [84]. Other methods, such as electrospinning [198], CVD [199], templating [200], etching [201], template-assisted electrodeposition [195], photolithography [202], and colloidal lithography-plasma texturing [203] have also been used to create re-entrant structures. However, most of these methods are complex and costly, and require expensive equipment.

The most extensively studied method for generating MD membranes with re-entrant structures and low surface energy involves nanoparticle coating of nanofibrous membranes, followed by surface fluorination [204]. Electrospun hollow fibers can provide re-entrant structures on the bottom-half of the electrospun fibrous networks [205]. However, post-modification methods with nanoparticles and fluorinating agents are required to lower the surface energy and provide a more re-entrant structure. Successful fabrication of omniphobic MD membranes has been achieved by coating hydrophobic polymers (e.g. PVDF [170] and PVDF-HFP nanofibers [172]) with silica nanoparticles, followed by fluorination using materials such as FAS17 [170], Teflon AF 2400 [206] and fluoroalkylsilane [172]. To ensure a stable flux and an outstanding rejection, a chemical binding agent is often used to enhance the adhesion between the coating and the membrane substrate [170]. In addition, the one-step incorporation of fluorodecyl polyhedral oligomeric silsesquioxane was also able to reduce the surface energy and create a re-entrant beads-on-string structure [84,205].

LBL assembly is a proven method to engineer re-entrant structures [93,170]. The process involves four steps: (1) membrane surface functionalization/pre-treatment to improve nanoparticle attachment,

(2) nanoparticle coating, (3) polymer solution coating to stabilize the nanoparticle layer (e.g. silanization), and (4) fluorination. These steps are also often used to create superhydrophobic and/or omniphobic membranes with hierarchical and/or re-entrant structures. For example, Zheng et al. pre-treated the surface of a PVDF membrane with an alkaline solution, and then coated it with APTES solution [170]. The prepared polystyrene microspheres by free radical dispersion polymerization were applied to create a coating layer on silica nanoparticles. The silica-polystyrene microspheres dispersed in alcohol were spray-coated onto the APTES modified PVDF membrane. The prepared membrane was fluorinated with FAS17, and exhibited re-entrant structures with water and hexane CAs of 176° and 138° , respectively.

5. Green modification materials/methods

Hydrophobicity is a key factor in the performance of MD membranes and a plethora of research has been done to enhance membrane hydrophobicity as discussed in previous sections. However, most of the hydrophobic modifications are based on expensive and potentially hazardous fluorination materials that may cause severe environmental and health issues due to their persistent and bioaccumulation nature [103,207,208]. Therefore, fabricating hydrophobic membranes without using fluoride-containing compounds is highly desirable to reduce membrane costs and minimize the related environmental and health risks [52]. Several alternative strategies have been explored to create re-entrant surfaces with low surface energy, including modification with alkyl functional groups, carbon-based materials, and polymerization/copolymerization. Table 5 summarizes the studies on the surface modification of MD membranes without using fluoride-containing materials.

Alkyl functionalization of silanes and nanoparticles such as SiO_2 , TiO_2 , ZnO , etc. is an effective method to enhance the hydrophobicity of MD membranes. For successful modification with alkyl silane solutions, the membrane surface should contain functional groups (e.g., hydroxyl or amino) to react with trichloride or trialkoxy groups of the alkyl silanes. For instance, ceramic membranes with hydroxyl groups on the surface were easily modified with an n-octyltriethoxysilane agent and became highly hydrophobic [159]. Alkyl modifying agents such as alkylsilanes and alkyl phosphonic acids have been used to modify nanoparticles. For example, hexadecyltrimethoxysilane agent was used to modify the surface of SiO_2 coated PVDF membrane, creating a re-entrant structure [211]. The fabricated membranes exhibited an enhanced WCA of 141.6° and the flux was four times higher than that of the pristine PVDF membranes. In another study, micron-sized silica particles were modified by grafting spherical polyvinylsilsesquioxane nanoparticles onto them [218]. The hydrophobic groups including vinyls and methoxyls enabled a superhydrophobic membrane surface

Table 5
Modification of MD membranes with non-fluoroalkyl materials.

Polymer	Nanomaterial	Non-fluoro modifier	Feed T (°C)	Permeate T (°C)	Feed salinity (g•L ⁻¹)	WCA (°)	LEP (bar)	Flux (kg•m ⁻² •h ⁻¹)	Rejection (%)	Ref.
PVDF-HFP	CNF	Glutaraldehyde crosslinked with collagen	70	20	30	113	–	8.1	99.8	[209]
PVDF	–	n-Octyltriethoxysilane				121	6.4	5.5	–	[210]
PVDF	SiO ₂	Hexadecyltrimethoxysilane	50	20	58.44	142	2.64	8.0	–	[211]
PVDF	ZnO	3-Aminopropyltriethoxysilane/lauric acid	86	22	12–13	71	7.5	25	99	[212]
PVDF	GO	3-(Aminopropyl)triethoxysilane	85	20	35	78	–	6.2	>99.9	[213]
PES/PVDF	GO	Hydrocarbon modified graphene nanoplatelets	65	25	10	132	0.85	19.4	–	[214]
BPs	CNTs	3-Glycidoxypropyltrimethoxysilane	55, 75	5	35	140	4.41	8.3	98.3	[215]
BPs	CNTs	Polystyrene	70	5	35	95	–	15.0	95	[216]
PET	CNTs	Triethoxyvinylsilane	85	10	30	104	4.3	0.7	99.3	[217]
TeMs										
PVDF	SiO ₂	Polyvinylsilsesquioxane/vinyltrimethoxysilane	53	20	35	160	3.53	9.8	100	[218]
PVC	–	Polyethylacrylate	45–65	20	35–200	96	–	30	99.9	[219]

(WCA 160°) with low surface energy and the LEP of the modified membrane was 3.53 bar [218].

Carbon-based materials are cheaper and less toxic compared with fluorine-containing compounds. Chemicals without fluoride often have lower costs than chemicals containing this element [52]. Moreover, some carbon-based materials are highly hydrophobic and can be used to fabricate hydrophobic MD membranes [52]. Therefore, they are excellent substitutions for fluorine-containing compounds in the modification of MD membranes.

Carbon-based materials, such as diamond, graphite, activated carbon, carbon nanotubes (CNTs), graphene, or carbon quantum dots have been used to modify MD membranes due to their inherent hydrophobicity [220]. Hydrophobic activated carbon materials with good adsorptive properties were mixed with PVDF-HFP dope solution to fabricate MD membranes via electrospinning, increasing in both WCA and permeate flux [221]. Electrospinning of reduced graphene oxide (GO) and PVDF-HFP has also been shown to enhance the membrane hydrophobicity [222]. Moreover, the hydrophobicity of the reduced GO can be further increased by grafting alkyl chains to the polar functional groups of the material surface containing oxygen and hydrogen [214]. CNTs have high permeability, and excellent mechanical, thermal, and superhydrophobic properties, making them promising candidates for MD membrane modification [101,223]. However, the fabricated membranes suffer from cracks due to the weak interaction between the nanotubes, which could be solved by the integration of hydrophobic polymers (e.g., polypropylene and PVDF). For MD membrane fabrication with carbon-based materials, flux enhancement is a popular research direction in this area due to the special features of carbon materials [224,225].

Another method to enhance the hydrophobicity of the MD membrane surface is the utilization of polymerization or copolymerization reactions to produce polymers containing nonpolar hydrocarbon chains [218,226]. In such reactions, the monomers often have double bonds or other functional groups such as alkyl chains and silanes. In addition, the substrate material should contain or be pre-treated to contain active functional groups, such as double bonds to react with the monomers [52].

Surface fluorination is a very common method to engineer antiwetting hydrophobic, superhydrophobic or omniphobic MD membranes [45,79,227]. However, economic and environmental issues with fluoride-containing materials call for greener, more sustainable and cost-effective fabrication materials and methods for MD membranes. Carbon-based materials have emerged as a promising option for creating fluoride-free membranes that exhibit high stability and hydrophobicity. While the literature demonstrates the technical feasibility of creating fluorocarbon-free superhydrophobic or omniphobic membranes,

challenges still exist in achieving the same level of mechanical stability and chemical inertness as fluorinated membranes. Nonetheless, the development of such membranes will not only improve the MD membrane performance, but also address the need for environmentally-friendly and cost-effective membranes in various industries.

6. Concluding remarks and prospects

MD is a non-isothermal process that has been widely used for desalination, wastewater treatment and volatile resource recovery. It is promising in treating hypersaline and oily liquid streams due to its special separation mechanism, low mechanical requirement, and capability of operating with a low-grade heat source. However, some challenges, such as pore wetting and membrane fouling limit its commercialization. Engineering antiwetting hydrophobic surfaces has shown great promise in enhancing the efficiency and durability of MD. A systematic approach to mitigate wetting is to enhance the liquid entry pressure (LEP) of the membrane by surface engineering. The key antiwetting engineering strategies include decreasing the maximum membrane pore size, minimizing the membrane surface free energy, and creating rough surfaces with hierarchical/re-entrant structures.

Pore size reduction enhances the LEP but reduces permeate flux at the same time, suggesting the importance of optimizing the pore size distribution. Surface modification methods, such as coating (with inorganic nanoparticles and/or hydrophobic polymers), vapor deposition, and layer-by-layer (LbL) assembly have been applied to effectively reduce the pore size, followed by a fluorination step to further enhance the membrane hydrophobicity. Phase inversion and electrospinning methods have been used to prepare MD membranes. Synthesis conditions and polymer selection can be optimized to achieve a high LEP along with a narrow sponge-like structure and high mechanical strength for the membrane.

Surface energy reduction is an effective way to increase the surface hydrophobicity, LEP, and thus antiwetting performance of a hydrophobic membrane by altering the surface chemistry. It can be achieved by incorporating low surface energy materials (e.g., hydrophobic polymers) in the membrane matrix or coating/grafting low surface energy materials (e.g., fluorosilanes) on the membrane surface. The commonly used hydrophobic functional groups are $-CH_3$, $-CH_2-CH_2-$, and $-CF_3$. Fluorination, mostly on nanoparticle-coated MD membranes, is another effective method to enhance the membrane hydrophobicity and roughness.

Surface roughness enhancement by creating single/multi-level hierarchical or re-entrant structures on the membrane surface is another common method to increase the CA, LEP and thus the antiwetting performance of a hydrophobic membrane. Hierarchical nano-/micro-

structures with multi-level roughness can be prepared by electrospinning, fluorination, LbL assembly, or incorporation of inorganic metalloids and metal oxides (e.g., SiO₂, TiO₂, ZnO, and Al₂O₃). Re-entrant structures can be introduced in various geometries such as micro-mushrooms, micro-hoodoo arrays, and nanoparticle coatings via top-down or bottom-up techniques such as lithography, electrospinning, chemical vapor deposition, template technique, etching, and photolithography. Creating re-entrant structures provides a high CA surface with a Cassie-Baxter state.

Economic and environmental issues associated with fluoride-containing materials have driven research into the fabrication of green, sustainable, and more cost-effective membranes without fluoride-containing compounds. The main alternative strategies for engineering antiwetting membranes include the incorporation of alkyl functional groups, modification with carbon-based materials, and polymerization/copolymerization. Carbon-based materials are promising fluoride-free materials that exhibit high stability and hydrophobicity. However, there are still challenges in fabricating carbon-based membranes with high mechanical stability and chemical inertness.

To achieve commercialization of MD, there are still many obstacles to overcome, particularly the wetting issue. The first key challenge is the trade-off between the membrane permeability and wetting resistance. Antiwetting MD membranes often have small pore sizes that lead to low membrane permeability. High-flux MD membranes usually have low long-term stabilities due to their low wetting resistance. To enhance the antiwetting properties of MD membranes, various coating/modification materials (e.g. nanoparticles, nanosheets and nanotubes) and methods have been employed. However, their costs, environmental impacts and stabilities in the long run are still unclear and thus need further investigations before large-scale adoption. In practical MD applications, the feed solution may be highly complex, such as containing surfactants and/or corrosive substances, and the feed properties (e.g. surface tension) may significantly vary with the temperature, leading to complicated interactions (e.g. concentration polarization) between the feed solution and the membrane surface. In addition, the coating materials often have different thermal conductivities with the polymer membranes. How the coating materials affect the temperature polarization in MD would be an interesting question to explore. In the future, more research efforts should be made to these areas before MD can be commercialized at large scale.

Moving forward, engineering antiwetting hydrophobic surfaces for MD applications will continue to be an active area of research, with a focus on improving the durability and stability of these membranes, improving the scalability of the fabrication methods, and reducing the fabrication cost. In addition, there is a need to further explore more environmental-friendly materials for membrane antiwetting modification.

Finally, the integration of antiwetting membranes with other processes may also hold great promise for the development of more efficient and sustainable water treatment processes. Overall, the future looks bright for the continued development and application of antiwetting hydrophobic MD membranes for high salinity challenging waste liquid treatment, zero liquid discharge and resource recovery.

Declaration of competing interest

The authors declare that they have no known competing financial interests or personal relationships that could have appeared to influence the work reported in this paper.

Data availability

Data will be made available on request.

Acknowledgments

The financial support from the Australian Research Council (ARC) Discovery Project (DP230100307) is acknowledged.

References

- [1] S. Kalla, K.S. Piash, O. Sanyal, Anti-fouling and anti-wetting membranes for membrane distillation, *J. Water Process Eng.* 46 (2022), 102634.
- [2] S. Zhao, Q. Zeng, C.-C. Wang, Editorial: inorganic materials for energy and environmental applications, *Front. Chem.* 10 (2022).
- [3] A. Samadi, M. Xie, J. Li, H. Shon, C. Zheng, S. Zhao, Polyaniline-based adsorbents for aqueous pollutants removal: a review, *Chem. Eng. J.* 418 (2021), 129425.
- [4] D.Q. Zhang, W.L. Zhang, Y.N. Liang, Adsorption of perfluoroalkyl and polyfluoroalkyl substances (PFASs) from aqueous solution - a review, *Sci. Total Environ.* 694 (2019), 133606.
- [5] X. Zhang, J. Lin, W. Ye, W. Zhou, X. Jia, S. Zhao, C. Ye, Potential of coagulation/GAC adsorption combined with UV/H₂O₂ and ozonation for removing dissolved organic matter from secondary RO concentrate, *J. Chem. Technol. Biotechnol.* 94 (2019) 1091–1099.
- [6] H. Kuang, Z. He, M. Li, R. Huang, Y. Zhang, X. Xu, L. Wang, Y. Chen, S. Zhao, Enhancing co-catalysis of MoS₂ for persulfate activation in Fe³⁺-based advanced oxidation processes via defect engineering, *Chem. Eng. J.* 127987 (2020).
- [7] J. Fu, P. Gao, L. Wang, Y. Zhang, Y. Deng, R. Huang, S. Zhao, Z. Yu, Y. Wei, G. Wang, S. Zhou, Regulating crystal facets of MnO₂ for enhancing peroxymonosulfate activation to degrade pollutants: performance and mechanism, *Catalysts* 12 (2022) 342.
- [8] Q. Zeng, Y. Wang, Q. Zhang, J. Hu, Y. Wen, J. Wang, R. Wang, S. Zhao, Activity and mechanism of vanadium sulfide for organic contaminants oxidation with peroxymonosulfate, *J. Colloid Interface Sci.* 635 (2023) 358–369.
- [9] S. Zhao, M. Golestani, A. Penesyan, B. Deng, C. Zheng, V. Strezov, Antibiotic enhanced dopamine polymerization for engineering antifouling and antimicrobial membranes, *Chin. Chem. Lett.* 31 (2020) 851–854.
- [10] S. Lin, H. Zhao, L. Zhu, T. He, S. Chen, C. Gao, L. Zhang, Seawater desalination technology and engineering in China: a review, *Desalination* 498 (2021), 114728.
- [11] S. Zhao, Z. Liao, A. Fane, J. Li, C. Tang, C. Zheng, J. Lin, L. Kong, Engineering antifouling reverse osmosis membranes: a review, *Desalination* 499 (2021), 114857.
- [12] A. Samadi, S. Zhao, Q. Fu, G. Yi, Supramolecular membranes for liquid separation, in: *Advances in Functional Separation Membranes*, 2021, p. 232.
- [13] F. Nabeel, T. Rasheed, M. Bilal, H.M. Iqbal, Supramolecular membranes: a robust platform to develop separation strategies towards water-based applications, *Sep. Purif. Technol.* 215 (2019) 441–453.
- [14] O.S. Ekande, M. Kumar, Review on polyaniline as reductive photocatalyst for the construction of the visible light active heterojunction for the generation of reactive oxygen species, *J. Environ. Chem. Eng.* 105725 (2021).
- [15] A. Samadi, S. Zhao, Polyaniline-based adsorbents and photocatalysts for the elimination of toxic heavy metals, in: *Advanced Materials for a Sustainable Environment*, CRC Press, 2022, pp. 101–122.
- [16] Z. He, S. Mahmud, Y. Yang, L. Zhu, Y. Zhao, Q. Zeng, Z. Xiong, S. Zhao, Polyvinylidene fluoride membrane functionalized with zero valent iron for highly efficient degradation of organic contaminants, *Sep. Purif. Technol.* 250 (2020), 117266.
- [17] C. Li, G. Feng, Z. Pan, C. Song, X. Fan, P. Tao, T. Wang, M. Shao, S. Zhao, High-performance electrocatalytic microfiltration CuO/Carbon membrane by facile dynamic electrodeposition for small-sized organic pollutants removal, *J. Membr. Sci.* 601 (2020), 117913.
- [18] S. Sahebi, M. Kahrizi, N. Fadaie, S. Hadadpour, B. Ramavandi, R.R. Gonzales, Developing a thin film composite membrane with hydrophilic sulfonated substrate on nonwoven backing fabric support for forward osmosis, *Membranes* 11 (2021) 813.
- [19] M. Kahrizi, N. Kasiri, T. Mohammadi, S. Zhao, Introducing sorption coefficient through extended UNIQUAC and Flory-Huggins models for improved flux prediction in forward osmosis, *Chem. Eng. Sci.* 198 (2019) 33–42.
- [20] S. Zhou, F. Liu, J. Wang, H. Lin, Q. Han, S. Zhao, C.Y. Tang, Janus membrane with unparalleled forward osmosis performance, *Environ. Sci. Technol. Lett.* 6 (2019) 79–85.
- [21] Ramato A. Tufa, E. Curcio, E. Brauns, W. van Baak, E. Fontananova, G. Di Profio, Membrane distillation and reverse electro dialysis for near-zero liquid discharge and low energy seawater desalination, *J. Membr. Sci.* 496 (2015) 325–333.
- [22] S. Zhao, L. Shen, Editorial: advanced membrane science and technology for sustainable environmental applications, *Front. Chem.* 8 (2020).
- [23] Q. He, G. Yu, T. Tu, S. Yan, Y. Zhang, S. Zhao, Closing CO₂ loop in biogas production: recycling ammonia as fertilizer, *Environ. Sci. Technol.* 51 (2017) 8841–8850.
- [24] M. Essalhi, M. Khayet, Chapter three - membrane distillation (MD), in: S. Tarleton (Ed.), *Progress in Filtration and Separation*, Academic Press, Oxford, 2015, pp. 61–99.
- [25] S. Lin, N.Y. Yip, T.Y. Cath, C.O. Osuji, M. Elimelech, Hybrid pressure retarded osmosis–membrane distillation system for power generation from low-grade heat: thermodynamic analysis and energy efficiency, *Environ. Sci. Technol.* 48 (2014) 5306–5313.

- [26] Y.-R. Chen, R. Xin, X. Huang, K. Zuo, K.-L. Tung, Q. Li, Wetting-resistant photothermal nanocomposite membranes for direct solar membrane distillation, *J. Membr. Sci.* 620 (2021), 118913.
- [27] X. Zhu, Y. Liu, F. Du, J. Han, G. Hao, L. Li, Q. Ma, Geothermal direct contact membrane distillation system for purifying brackish water, *Desalination* 500 (2021), 114887.
- [28] K.S. Christie, T. Horseman, S. Lin, Energy efficiency of membrane distillation: simplified analysis, heat recovery, and the use of waste-heat, *Environ. Int.* 138 (2020), 105588.
- [29] A. Alkudhri, N. Darwish, N. Hilal, Membrane distillation: a comprehensive review, *Desalination* 287 (2012) 2–18.
- [30] S. Zhao, P.H.M. Feron, X. Chen, I. Boztepe, J. Zhang, N.R. Mirza, L. Kong, Gas flow enhanced mass transfer in vacuum membrane distillation, *Desalination* 552 (2023), 116434.
- [31] S. Zhao, P.H.M. Feron, C. Cao, L. Wardhaugh, S. Yan, S. Gray, Membrane evaporation of amine solution for energy saving in post-combustion carbon capture: Wetting and condensation, *Sep. Purif. Technol.* 146 (2015) 60–67.
- [32] S. Sinha Ray, H.-K. Lee, Y.-N. Kwon, Review on blueprint of designing anti-wetting polymeric membrane surfaces for enhanced membrane distillation performance, *Polymers* 12 (2020) 23.
- [33] H. Chamani, J. Woloszyn, T. Matsuura, D. Rana, C.Q. Lan, Pore wetting in membrane distillation: a comprehensive review, *Prog. Mater. Sci.* 122 (2021), 100843.
- [34] A. Figoli, S. Santoro, F. Galiano, A. Basile, Pervaporation membranes: preparation, characterization, and application, in: *Pervaporation, Vapour Permeation and Membrane Distillation*, Elsevier, 2015, pp. 19–63.
- [35] S. Zhao, P.H.M. Feron, Z. Xie, J. Zhang, M. Hoang, Condensation studies in membrane evaporation and sweeping gas membrane distillation, *J. Membr. Sci.* 462 (2014) 9–16.
- [36] L. Eykens, K. De Sitter, C. Dotremont, L. Pinoy, B. Van der Bruggen, Membrane synthesis for membrane distillation: a review, *Sep. Purif. Technol.* 182 (2017) 36–51.
- [37] Y. Chen, Z. Wang, G.K. Jennings, S. Lin, Probing pore wetting in membrane distillation using impedance: early detection and mechanism of surfactant-induced wetting, *Environ. Sci. Technol. Lett.* 4 (2017) 505–510.
- [38] M.R. Choudhury, N. Anwar, D. Jassby, M.S. Rahaman, Fouling and wetting in the membrane distillation driven wastewater reclamation process – a review, *Adv. Colloid Interf. Sci.* 269 (2019) 370–399.
- [39] E. Drioli, A. Ali, F. Macedonio, Membrane distillation: recent developments and perspectives, *Desalination* 356 (2015) 56–84.
- [40] A. Alkudhri, N. Darwish, N. Hilal, Membrane distillation: a comprehensive review, *Desalination* 287 (2012) 2–18.
- [41] S. Zhao, S. Hu, X. Zhang, L. Song, Y. Wang, M. Tan, L. Kong, Y. Zhang, Integrated membrane system without adding chemicals for produced water desalination towards zero liquid discharge, *Desalination* 114693 (2020).
- [42] S.S. Ray, S.-S. Chen, D. Sangeetha, H.-M. Chang, C.N.D. Thanh, Q.H. Le, H.-M. Ku, Developments in forward osmosis and membrane distillation for desalination of waters, *Environ. Chem. Lett.* 16 (2018) 1247–1265.
- [43] M. Rezaei, D.M. Warsinger, J.H. Lienhard V, M.C. Duke, T. Matsuura, W. M. Samhaber, Wetting phenomena in membrane distillation: mechanisms, reversal, and prevention, *Water Res.* 139 (2018) 329–352.
- [44] Y. Zhang, X. Wang, Z. Cui, E. Drioli, Z. Wang, S. Zhao, Enhancing wetting resistance of poly(vinylidene fluoride) membranes for vacuum membrane distillation, *Desalination* 415 (2017) 58–66.
- [45] Z. Xiong, Q. Lai, J. Lu, F. Qu, H. Yu, X. Chen, G. Zhang, W. Zhang, S. Zhao, Silanization enabled superhydrophobic PTFE membrane with antiwetting and antifouling properties for robust membrane distillation, *J. Membr. Sci.* 674 (2023), 121546.
- [46] T. Ni, J. Lin, L. Kong, S. Zhao, Omniphobic membranes for distillation: opportunities and challenges, *Chin. Chem. Lett.* 32 (2021) 3298–3306.
- [47] A. Abdel-Karim, S. Leaper, C. Skuse, G. Zaragoza, M. Gryta, P. Gorgojo, Membrane cleaning and pretreatments in membrane distillation—a review, *Chem. Eng. J.* 422 (2021), 129696.
- [48] E. Arjmand, A. Mansourizadeh, A.M. Ghaedi, M. Rahbari-Sisakht, Surface modification of porous polyvinylidene fluoride hollow fiber membrane by sulfonated poly(ether ether ketone) coating for membrane distillation of oily wastewater, *J. Appl. Polym. Sci.* 139 (2022), e53196.
- [49] K. Wang, D. Hou, J. Wang, Z. Wang, B. Tian, P. Liang, Hydrophilic surface coating on hydrophobic PTFE membrane for robust anti-oil-fouling membrane distillation, *Appl. Surf. Sci.* 450 (2018) 57–65.
- [50] K. Karakulski, M. Gryta, Water demineralisation by NF/MD integrated processes, *Desalination* 177 (2005) 109–119.
- [51] K.J. Lu, Y. Chen, T.-S. Chung, Design of omniphobic interfaces for membrane distillation – a review, *Water Res.* 162 (2019) 64–77.
- [52] H.T. Nguyen, H.M. Bui, Y.-F. Wang, S.-J. You, Non-fluoroalkyl functionalized hydrophobic surface modifications used in membrane distillation for cheaper and more environmentally friendly applications: a mini-review, *Sustain. Chem. Pharm.* 28 (2022), 100714.
- [53] H.B. Madalosso, R. Machado, D. Hotza, C. Marangoni, Membrane surface modification by electrospinning, coating, and plasma for membrane distillation applications: a state-of-the-art review, *Adv. Eng. Mater.* 23 (2021), 2001456.
- [54] W.A.F.W. AbdulKadir, A.L. Ahmad, O.B. Seng, N.F.C. Lah, Biomimetic hydrophobic membrane: a review of anti-wetting properties as a potential factor in membrane development for membrane distillation (MD), *J. Ind. Eng. Chem.* 91 (2020) 15–36.
- [55] M. Yao, L.D. Tijing, G. Naidu, S.-H. Kim, H. Matsuyama, A.G. Fane, H.K. Shon, A review of membrane wettability for the treatment of saline water deploying membrane distillation, *Desalination* 479 (2020), 114312.
- [56] M.K. Alsebaei, A.L. Ahmad, Membrane distillation: progress in the improvement of dedicated membranes for enhanced hydrophobicity and desalination performance, *J. Ind. Eng. Chem.* 86 (2020) 13–34.
- [57] M. Gryta, Long-term performance of membrane distillation process, *J. Membr. Sci.* 265 (2005) 153–159.
- [58] M.R. Qtaishat, T. Matsuura, 13 - modelling of pore wetting in membrane distillation compared with pervaporation, in: A. Basile, A. Figoli, M. Khayet (Eds.), *Pervaporation, Vapour Permeation and Membrane Distillation*, Woodhead Publishing, Oxford, 2015, pp. 385–413.
- [59] S. Mosadegh-Sedghi, D. Rodrigue, J. Brisson, M.C. Iliuta, Wetting phenomenon in membrane contactors – causes and prevention, *J. Membr. Sci.* 452 (2014) 332–353.
- [60] A.M. Alkhalabi, N. Lior, Membrane-distillation desalination: status and potential, *Desalination* 171 (2005) 111–131.
- [61] C. Gostoli, G.C. Sarti, S. Matulli, Low temperature distillation through hydrophobic membranes, *Sep. Sci. Technol.* 22 (1987) 855–872.
- [62] X. Yang, R. Wang, L. Shi, A.G. Fane, M. Debowski, Performance improvement of PVDF hollow fiber-based membrane distillation process, *J. Membr. Sci.* 369 (2011) 437–447.
- [63] H. Zhu, H. Wang, F. Wang, Y. Guo, H. Zhang, J. Chen, Preparation and properties of PTFE hollow fiber membranes for desalination through vacuum membrane distillation, *J. Membr. Sci.* 446 (2013) 145–153.
- [64] J.-M. Li, Z.-K. Xu, Z.-M. Liu, W.-F. Yuan, H. Xiang, S.-Y. Wang, Y.-Y. Xu, Microporous polypropylene and polyethylene hollow fiber membranes. Part 3. Experimental studies on membrane distillation for desalination, *Desalination* 155 (2003) 153–156.
- [65] M. Gryta, Influence of polypropylene membrane surface porosity on the performance of membrane distillation process, *J. Membr. Sci.* 287 (2007) 67–78.
- [66] Z. Wang, Y. Chen, S. Lin, Kinetic model for surfactant-induced pore wetting in membrane distillation, *J. Membr. Sci.* 564 (2018) 275–288.
- [67] G. Dong, J.F. Kim, J.H. Kim, E. Drioli, Y.M. Lee, Open-source predictive simulators for scale-up of direct contact membrane distillation modules for seawater desalination, *Desalination* 402 (2017) 72–87.
- [68] I. Hitsov, T. Maere, K. De Sitter, C. Dotremont, I. Nopens, Modelling approaches in membrane distillation: a critical review, *Sep. Purif. Technol.* 142 (2015) 48–64.
- [69] L. Peña, J.M.O. de Zárate, J.I. Mengual, Steady states in membrane distillation: influence of membrane wetting, *J. Chem. Soc. Faraday Trans.* 89 (1993) 4333–4338.
- [70] M.C. García-Payo, M.A. Izquierdo-Gil, C. Fernández-Pineda, Wetting study of hydrophobic membranes via liquid entry pressure measurements with aqueous alcohol solutions, *J. Colloid Interface Sci.* 230 (2000) 420–431.
- [71] L. Eykens, K. De Sitter, C. Dotremont, L. Pinoy, B. Van der Bruggen, How to optimize the membrane properties for membrane distillation: a review, *Ind. Eng. Chem. Res.* 55 (2016) 9333–9343.
- [72] T. Young, *A Course of Lectures on Natural Philosophy and the Mechanical Arts: In Two Volumes*, Johnson, 1807.
- [73] A.C.M. Franken, J.A.M. Nolten, M.H.V. Mulder, D. Bargeman, C.A. Smolders, Wetting criteria for the applicability of membrane distillation, *J. Membr. Sci.* 33 (1987) 315–328.
- [74] R.B. Saffarini, B. Mansoor, R. Thomas, H.A. Arafat, Effect of temperature-dependent microstructure evolution on pore wetting in PTFE membranes under membrane distillation conditions, *J. Membr. Sci.* 429 (2013) 282–294.
- [75] W.R. Purcell, Interpretation of capillary pressure data, *J. Pet. Technol.* 2 (1950) 11–12.
- [76] A.T. Servi, J. Kharraz, D. Klee, K. Notarangelo, B. Eyob, E. Guillen-Burrieza, A. Liu, H.A. Arafat, K.K. Gleason, A systematic study of the impact of hydrophobicity on the wetting of MD membranes, *J. Membr. Sci.* 520 (2016) 850–859.
- [77] H. Chamani, P. Yazgan-Birgi, T. Matsuura, D. Rana, M.I. Hassan Ali, H.A. Arafat, C.Q. Lan, CFD-based genetic programming model for liquid entry pressure estimation of hydrophobic membranes, *Desalination* 476 (2020), 114231.
- [78] Z. Zhu, L. Zhong, T. Horseman, Z. Liu, G. Zeng, Z. Li, S. Lin, W. Wang, Superhydrophobic-omniphobic membrane with anti-deformable pores for membrane distillation with excellent wetting resistance, *J. Membr. Sci.* 620 (2021), 118768.
- [79] W. Zhang, Y. Lu, J. Liu, X. Li, B. Li, S. Wang, Preparation of re-entrant and anti-fouling PVDF composite membrane with omniphobicity for membrane distillation, *J. Membr. Sci.* 595 (2020), 117563.
- [80] L. Eykens, K. De Sitter, C. Dotremont, L. Pinoy, B. Van der Bruggen, Coating techniques for membrane distillation: an experimental assessment, *Sep. Purif. Technol.* 193 (2018) 38–48.
- [81] R.N. Wenzel, Resistance of solid surfaces to wetting by water, *Ind. Eng. Chem.* 28 (1936) 988–994.
- [82] A.B.D. Cassie, S. Baxter, Wettability of porous surfaces, *Trans. Faraday Soc.* 40 (1944) 546–551.
- [83] D. Wang, Q. Sun, M.J. Hokkanen, C. Zhang, F.-Y. Lin, Q. Liu, S.-P. Zhu, T. Zhou, Q. Chang, B. He, Q. Zhou, L. Chen, Z. Wang, R.H.A. Ras, X. Deng, Design of robust superhydrophobic surfaces, *Nature* 582 (2020) 55–59.
- [84] A. Tuteja, W. Choi, M. Ma, J.M. Mabry, S.A. Mazzella, G.C. Rutledge, G. H. McKinley, R.E. Cohen, Designing superoleophobic surfaces, *Science* 318 (2007) 1618–1622.

- [85] J. Ju, K. Fejjari, Y. Cheng, M. Liu, Z. Li, W. Kang, Y. Liao, Engineering hierarchically structured superhydrophobic PTFE/POSS nanofibrous membranes for membrane distillation, *Desalination* 486 (2020), 114481.
- [86] A. Samadi, A.H. Navarchian, Matrimid–polyaniline/clay mixed-matrix membranes with plasticization resistance for separation of CO₂ from natural gas, *Polym. Adv. Technol.* 27 (2016) 1228–1236.
- [87] K. Schneider, W. Hölz, R. Wollbeck, S. Ripperger, Membranes and modules for transmembrane distillation, *J. Membr. Sci.* 39 (1988) 25–42.
- [88] S. Zhao, L. Zou, Relating solution physicochemical properties to internal concentration polarization in forward osmosis, *J. Membr. Sci.* 379 (2011) 459–467.
- [89] B.S. Lalia, E. Guillen, H.A. Arafat, R. Hashaikeh, Nanocrystalline cellulose reinforced PVDF-HFP membranes for membrane distillation application, *Desalination* 332 (2014) 134–141.
- [90] H. Ji, M. Gu, G. Zhang, C. Yue, Z. Yuan, D. Liu, S. Shen, X. Zhou, I. Wyman, Janus membrane prepared via one step depositing coatings onto PVDF/PDMS membrane for simultaneous antiwetting and antifouling in DCMD, *Desalination* 539 (2022), 115964.
- [91] F. Guo, A. Servi, A. Liu, K.K. Gleason, G.C. Rutledge, Desalination by membrane distillation using electrospun polyamide fiber membranes with surface fluorination by chemical vapor deposition, *ACS Appl. Mater. Interfaces* 7 (2015) 8225–8232.
- [92] Y. Chul Woo, Y. Chen, L.D. Tijing, S. Phuntho, T. He, J.-S. Choi, S.-H. Kim, H. Kyong Shon, CF₄ plasma-modified omniphobic electrospun nanofiber membrane for produced water brine treatment by membrane distillation, *J. Membr. Sci.* 529 (2017) 234–242.
- [93] Y.C. Woo, Y. Kim, M. Yao, L.D. Tijing, J.-S. Choi, S. Lee, S.-H. Kim, H.K. Shon, Hierarchical composite membranes with robust omniphobic surface using layer-by-layer assembly technique, *Environ. Sci. Technol.* 52 (2018) 2186–2196.
- [94] F. Tibi, A. Charfi, J. Cho, J. Kim, Fabrication of polymeric membranes for membrane distillation process and application for wastewater treatment: critical review, *Process Saf. Environ. Prot.* 141 (2020) 190–201.
- [95] J. Guo, B.J. Deka, K.-J. Kim, A.K. An, Regeneration of superhydrophobic TiO₂ electrospun membranes in seawater desalination by water flushing in membrane distillation, *Desalination* 468 (2019) 114054.
- [96] J. Zhang, Z. Song, B. Li, Q. Wang, S. Wang, Fabrication and characterization of superhydrophobic poly (vinylidene fluoride) membrane for direct contact membrane distillation, *Desalination* 324 (2013) 1–9.
- [97] Z. Wang, D. Hou, S. Lin, Composite membrane with underwater-oleophobic surface for anti-oil-fouling membrane distillation, *Environ. Sci. Technol.* 50 (2016) 3866–3874.
- [98] L.-F. Ren, F. Xia, V. Chen, J. Shao, R. Chen, Y. He, TiO₂-FTCS modified superhydrophobic PVDF electrospun nanofibrous membrane for desalination by direct contact membrane distillation, *Desalination* 423 (2017) 1–11.
- [99] P. Jiang, M.J. McFarland, Large-scale fabrication of wafer-size colloidal crystals, macroporous polymers and nanocomposites by spin-coating, *J. Am. Chem. Soc.* 126 (2004) 13778–13786.
- [100] L. Francis, N. Hilal, Electrospun CNTs on electrospun PVDF-Co-HFP membrane for robust membrane distillation, *Nanomaterials* 12 (2022) 4331.
- [101] L. Francis, N. Hilal, Electrohydrodynamic atomization of CNT on PTFE membrane for scaling resistant membranes in membrane distillation, *npj Clean Water* 6 (2023) 15.
- [102] X. Zhao, R. Zhang, Y. Liu, M. He, Y. Su, C. Gao, Z. Jiang, Antifouling membrane surface construction: chemistry plays a critical role, *J. Membr. Sci.* 551 (2018) 145–171.
- [103] X. Zhu, S. Feng, S. Zhao, F. Zhang, C. Xu, M. Hu, Z. Zhong, W. Xing, Perfluorinated superhydrophobic and oleophobic SiO₂@PTFE nanofiber membrane with hierarchical nanostructures for oily fume purification, *J. Membr. Sci.* 594 (2020), 117473.
- [104] Z. Cui, Y. Zhang, X. Li, X. Wang, E. Drioli, Z. Wang, S. Zhao, Optimization of novel composite membranes for water and mineral recovery by vacuum membrane distillation, *Desalination* 440 (2018) 39–47.
- [105] J. Zhao, K.K. Gleason, Solvent-less vapor-phase fabrication of membranes for sustainable separation processes, *Engineering* 6 (2020) 1432–1442.
- [106] M. Mohammadi Ghalehi, E. Tavakoli, M. Bavarian, S. Nejati, Fabricating Janus membranes via physicochemical selective chemical vapor deposition, *AIChE J.* 66 (2020), e17019.
- [107] J. Wang, X. Chen, R. Reis, Z. Chen, N. Milne, B. Winther-Jensen, L. Kong, L. F. Dumée, Plasma modification and synthesis of membrane materials—a mechanistic review, *Membranes* 8 (2018) 56.
- [108] X. Wei, B. Zhao, X.-M. Li, Z. Wang, B.-Q. He, T. He, B. Jiang, CF₄ plasma surface modification of asymmetric hydrophilic polyethersulfone membranes for direct contact membrane distillation, *J. Membr. Sci.* 407–408 (2012) 164–175.
- [109] C. Biloiu, I.A. Biloiu, Y. Sakai, H. Sugawara, A. Ohta, Amorphous fluorocarbon polymer (a-C:F) films obtained by plasma enhanced chemical vapor deposition from perfluoro-octane (C₈F₁₈) vapor. II. Dielectric and insulating properties, *J. Vac. Sci. Technol. A* 22 (2004) 1158–1165.
- [110] F.-X. Xiao, M. Pagliaro, Y.-J. Xu, B. Liu, Layer-by-layer assembly of versatile nanoarchitectures with diverse dimensionality: a new perspective for rational construction of multilayer assemblies, *Chem. Soc. Rev.* 45 (2016) 3088–3121.
- [111] Q. Long, S. Zhao, J. Chen, Z. Zhang, G. Qi, Z.-Q. Liu, Self-assembly enabled nano-intercalation for stable high-performance MXene membranes, *J. Membr. Sci.* 635 (2021), 119464.
- [112] N. Joseph, P. Ahmadiannamini, R. Hoogenboom, I.F.J. Vankelecom, Layer-by-layer preparation of polyelectrolyte multilayer membranes for separation, *Polym. Chem.* 5 (2014) 1817–1831.
- [113] G.-R. Xu, S.-H. Wang, H.-L. Zhao, S.-B. Wu, J.-M. Xu, L. Li, X.-Y. Liu, Layer-by-layer (LBL) assembly technology as promising strategy for tailoring pressure-driven desalination membranes, *J. Membr. Sci.* 493 (2015) 428–443.
- [114] A. Samadi, A.H. Navarchian, Separation of carbon dioxide from natural gas by matrimid-based mixed matrix membranes, *Gas Process. J.* 4 (2016) 1–18.
- [115] D. Hou, H. Fan, Q. Jiang, J. Wang, X. Zhang, Preparation and characterization of PVDF flat-sheet membranes for direct contact membrane distillation, *Sep. Purif. Technol.* 135 (2014) 211–222.
- [116] X. Liu, H. Liu, P. Li, Effect of Polymer Dope Concentration on the Morphology and Performance of PES/PDMS Hollow Fiber Composite Membrane for Gas Separation, 2017.
- [117] A. Samadi, L. Gao, L. Kong, Y. Orooji, S. Zhao, Waste-derived low-cost ceramic membranes for water treatment: opportunities, challenges and future directions, *Resour. Conserv. Recycl.* 185 (2022), 106497.
- [118] R. Thomas, E. Guillen-Burrieza, H.A. Arafat, Pore structure control of PVDF membranes using a 2-stage coagulation bath phase inversion process for application in membrane distillation (MD), *J. Membr. Sci.* 452 (2014) 470–480.
- [119] S.P. Deshmukh, K. Li, Effect of ethanol composition in water coagulation bath on morphology of PVDF hollow fiber membranes, *J. Membr. Sci.* 150 (1998) 75–85.
- [120] T. Young, An essay on the cohesion of fluids, *Philos. Trans. R. Soc.* 95 65–87.
- [121] D.K. Owens, R.C. Wendt, Estimation of the surface free energy of polymers, *J. Appl. Polym. Sci.* 13 (1969) 1741–1747.
- [122] Z. Chen, D. Rana, T. Matsuura, Y. Yang, C.Q. Lan, Study on the structure and vacuum membrane distillation performance of PVDF composite membranes: I. Influence of blending, *Sep. Purif. Technol.* 133 (2014) 303–312.
- [123] W. Wu, R.F. Giese Jr., C.J. van Oss, Evaluation of the Lifshitz-van der Waals/acid-base approach to determine surface tension components, *Langmuir* 11 (1995) 379–382.
- [124] M. Miwa, A. Nakajima, A. Fujishima, K. Hashimoto, T. Watanabe, Effects of the surface roughness on sliding angles of water droplets on superhydrophobic surfaces, *Langmuir* 16 (2000) 5754–5760.
- [125] J. Kujawa, W. Kujawski, Functionalization of ceramic metal oxide powders and ceramic membranes by perfluoroalkylsilanes and alkylsilanes possessing different reactive groups: physicochemical and tribological properties, *ACS Appl. Mater. Interfaces* 8 (2016) 7509–7521.
- [126] B.S. Lalia, V. Kochkodan, R. Hashaikeh, N. Hilal, A review on membrane fabrication: structure, properties and performance relationship, *Desalination* 326 (2013) 77–95.
- [127] N.A. Patankar, Mimicking the lotus effect: influence of double roughness structures and slender pillars, *Langmuir* 20 (2004) 8209–8213.
- [128] A. Razmjou, E. Arifin, G. Dong, J. Mansouri, V. Chen, Superhydrophobic modification of TiO₂ nanocomposite PVDF membranes for applications in membrane distillation, *J. Membr. Sci.* 415–416 (2012) 850–863.
- [129] W. Xu, T. Ning, X. Yang, S. Lu, Fabrication of superhydrophobic surfaces on zinc substrates, *Appl. Surf. Sci.* 257 (2011) 4801–4806.
- [130] S. Parvate, P. Dixit, S. Chattopadhyay, Superhydrophobic surfaces: insights from theory and experiment, *J. Phys. Chem. B* 124 (2020) 1323–1360.
- [131] B. Mandelbrot, How long is the coast of Britain? Statistical self-similarity and fractional dimension, *Science* 156 (1967) 636–638.
- [132] S. Shibuichi, T. Onda, N. Satoh, K. Tsujii, Super water-repellent surfaces resulting from fractal structure, *J. Phys. Chem.* 100 (1996) 19512–19517.
- [133] C. Boo, J. Lee, M. Elimelech, Omniphobic polyvinylidene fluoride (PVDF) membrane for desalination of shale gas produced water by membrane distillation, *Environ. Sci. Technol.* 50 (2016) 12275–12282.
- [134] Y. Peng, J. Ge, S. Wang, Z. Li, Occurrence of salt breakthrough and air-vapor pocket in a direct-contact membrane distillation, *Desalination* 402 (2017) 42–49.
- [135] M. Silvestrini, C. Brito, Wettability of reentrant surfaces: a global energy approach, *Langmuir* 33 (2017) 12535–12545.
- [136] N.A. Ahmad, C.P. Leo, A.L. Ahmad, W.K.W. Ramli, Membranes with great hydrophobicity: a review on preparation and characterization, *Sep. Purif. Rev.* 44 (2015) 109–134.
- [137] K. Szymczyk, B. Jańczuk, Surface tension of polytetrafluoroethylene and polymethyl methacrylate under the influence of the fluorocarbon surfactant film, *Ind. Eng. Chem. Res.* 51 (2012) 14076–14083.
- [138] G. Yi, X. Tang, L. Du, X. Li, S. Zhao, Hollow fiber polytetrafluoroethylene membrane heat exchanger with anti-corrosion properties, *J. Membr. Sci.* 678 (2023), 121664.
- [139] D. Sun, M.-Q. Liu, J.-H. Guo, J.-Y. Zhang, B.-B. Li, D.-Y. Li, Preparation and characterization of PDMS-PVDF hydrophobic microporous membrane for membrane distillation, *Desalination* 370 (2015) 63–71.
- [140] Z. Jin, D.L. Yang, S.H. Zhang, X.G. Jian, Hydrophobic modification of poly (phtalazinone ether sulfone ketone) hollow fiber membrane for vacuum membrane distillation, *J. Membr. Sci.* 310 (2008) 20–27.
- [141] L. Dumée, J.L. Campbell, K. Sears, J. Schütz, N. Finn, M. Duke, S. Gray, The impact of hydrophobic coating on the performance of carbon nanotube bucky-paper membranes in membrane distillation, *Desalination* 283 (2011) 64–67.
- [142] S. Lin, S. Nejati, C. Boo, Y. Hu, C.O. Osuji, M. Elimelech, Omniphobic membrane for robust membrane distillation, *Environ. Sci. Technol. Lett.* 1 (2014) 443–447.
- [143] J. Pan, C. Xiao, Q. Huang, H. Liu, J. Hu, ECTFE porous membranes with conveniently controlled microstructures for vacuum membrane distillation, *J. Mater. Chem. A* 3 (2015) 23549–23559.
- [144] L. Zheng, Z. Wu, Y. Zhang, Y. Wei, J. Wang, Effect of non-solvent additives on the morphology, pore structure, and direct contact membrane distillation performance of PVDF-CTFE hydrophobic membranes, *J. Environ. Sci.* 45 (2016) 28–39.

- [145] M. Khayet, C. Cojocaru, M. Essalhi, M.C. García-Payo, P. Arribas, L. García-Fernández, Hollow fiber spinning experimental design and analysis of defects for fabrication of optimized membranes for membrane distillation, *Desalination* 287 (2012) 146–158.
- [146] K. Chen, C. Xiao, Q. Huang, C. Zhang, Y. Wu, H. Liu, Z. Liu, Study on the fabrication and properties of FEP/SiO₂ hybrid flat-sheet membrane and its application in VMD, *Desalin. Water Treat.* 57 (2016) 14908–14918.
- [147] K. Chen, C. Xiao, Q. Huang, H. Liu, H. Liu, Y. Wu, Z. Liu, Study on vacuum membrane distillation (VMD) using FEP hollow fiber membrane, *Desalination* 375 (2015) 24–32.
- [148] C. Feng, B. Shi, G. Li, Y. Wu, Preparation and properties of microporous membrane from poly(vinylidene fluoride-co-tetrafluoroethylene) (F2.4) for membrane distillation, *J. Membr. Sci.* 237 (2004) 15–24.
- [149] J. Prince, D. Rana, G. Singh, T. Matsuura, T.J. Kai, T. Shanmugasundaram, Effect of hydrophobic surface modifying macromolecules on differently produced PVDF membranes for direct contact membrane distillation, *Chem. Eng. J.* 242 (2014) 387–396.
- [150] A. Mansourizadeh, Z. Aslmahdavi, A.F. Ismail, T. Matsuura, Blend polyvinylidene fluoride/surface modifying macromolecule hollow fiber membrane contactors for CO₂ absorption, *Int. J. Greenh. Gas Control* 26 (2014) 83–92.
- [151] H.T. Nguyen, M.-T. Pham, T.-M.T. Nguyen, H.M. Bui, Y.-F. Wang, S.-J. You, Modifications of conventional organic membranes with photocatalysts for antifouling and self-cleaning properties applied in wastewater filtration and separation processes: a review, *Sep. Sci. Technol.* 57 (2022) 1471–1500.
- [152] H. Trung Nguyen, S.-Y. Guo, S.-J. You, Y.-F. Wang, Visible light driven photocatalytic coating of PAA plasma-grafted PVDF membrane by TiO₂ doped with lanthanum recovered from waste fluorescent powder, *Environ. Eng. Res.* 27 (2022) (210144-210140).
- [153] F. Qu, A. Cao, Y. Yang, S. Mahmud, P. Su, J. Yang, Z. He, Q. Lai, L. Zhu, Z. Tu, Q. Wang, Z. Xiong, S. Zhao, Hierarchically superhydrophilic poly(vinylidene fluoride) membrane with self-cleaning fabricated by surface mineralization for stable separation of oily wastewater, *J. Membr. Sci.* 640 (2021), 119864.
- [154] Y. Liao, C.-H. Loh, R. Wang, A.G. Fane, Electrospun superhydrophobic membranes with unique structures for membrane distillation, *ACS Appl. Mater. Interfaces* 6 (2014) 16035–16048.
- [155] C. Yang, X.-M. Li, J. Gilron, D.-f. Kong, Y. Yin, Y. Oren, C. Linder, T. He, CF₄ plasma-modified superhydrophobic PVDF membranes for direct contact membrane distillation, *J. Membr. Sci.* 456 (2014) 155–161.
- [156] H. Shan, J. Liu, X. Li, Y. Li, F.H. Tezel, B. Li, S. Wang, Nanocoated amphiphobic membrane for flux enhancement and comprehensive anti-fouling performance in direct contact membrane distillation, *J. Membr. Sci.* 567 (2018) 166–180.
- [157] L.-H. Chen, A. Huang, Y.-R. Chen, C.-H. Chen, C.-C. Hsu, F.-Y. Tsai, K.-L. Tung, Omniphobic membranes for direct contact membrane distillation: effective deposition of zinc oxide nanoparticles, *Desalination* 428 (2018) 255–263.
- [158] L. Deng, H. Ye, X. Li, P. Li, J. Zhang, X. Wang, M. Zhu, B.S. Hsiao, Self-roughened omniphobic coatings on nanofibrous membrane for membrane distillation, *Sep. Purif. Technol.* 206 (2018) 14–25.
- [159] J. Kujawa, S. Al-Gharabli, W. Kujawski, K. Knozowska, Molecular grafting of fluorinated and nonfluorinated alkylsiloxanes on various ceramic membrane surfaces for the removal of volatile organic compounds applying vacuum membrane distillation, *ACS Appl. Mater. Interfaces* 9 (2017) 6571–6590.
- [160] Z. Xu, Z. Liu, P. Song, C. Xiao, Fabrication of super-hydrophobic polypropylene hollow fiber membrane and its application in membrane distillation, *Desalination* 414 (2017) 10–17.
- [161] Q. Liu, S. Huang, Y. Zhang, S. Zhao, Comparing the antifouling effects of activated carbon and TiO₂ in ultrafiltration membrane development, *J. Colloid Interface Sci.* 515 (2018) 109–118.
- [162] M. Kahrizi, R.R. Gonzales, L. Kong, H. Matsuyama, P. Lu, J. Lin, S. Zhao, Significant roles of substrate properties in forward osmosis membrane performance: a review, *Desalination* 528 (2022), 115615.
- [163] Z. He, S. Mahmud, S. Zhao, Y. Yang, L. Zhu, Y. Zhao, Q. Zeng, Z. Xiong, C. Hu, Hierarchically active poly(vinylidene fluoride) membrane fabricated by in situ generated zero-valent iron for fouling reduction, *ACS Appl. Mater. Interfaces* 12 (2020) 10993–11004.
- [164] Y. Wang, M. Han, L. Liu, J. Yao, L. Han, Beneficial CNT intermediate layer for membrane fluorination toward robust superhydrophobicity and wetting resistance in membrane distillation, *ACS Appl. Mater. Interfaces* 12 (2020) 20942–20954.
- [165] N. Dizge, E. Shaulsky, V. Karanikola, Electrospun cellulose nanofibers for superhydrophobic and oleophobic membranes, *J. Membr. Sci.* 590 (2019), 117271.
- [166] S.M. Seyed Shahabadi, H. Rabiee, S.M. Seyed, A. Mokhtare, J.A. Brant, Superhydrophobic dual layer functionalized titanium dioxide/polyvinylidene fluoride-co-hexafluoropropylene (TiO₂/PH) nanofibrous membrane for high flux membrane distillation, *J. Membr. Sci.* 537 (2017) 140–150.
- [167] J. Li, S. Guo, Z. Xu, J. Li, Z. Pan, Z. Du, F. Cheng, Preparation of omniphobic PVDF membranes with silica nanoparticles for treating coking wastewater using direct contact membrane distillation: electrostatic adsorption vs. chemical bonding, *J. Membr. Sci.* 574 (2019) 349–357.
- [168] X. Li, H. Shan, M. Cao, B. Li, Facile fabrication of omniphobic PVDF composite membrane via a waterborne coating for anti-wetting and anti-fouling membrane distillation, *J. Membr. Sci.* 589 (2019), 117262.
- [169] A.A. Khan, M.I. Siyal, C.-K. Lee, C. Park, J.-O. Kim, Hybrid organic-inorganic functionalized polyethersulfone membrane for hyper-saline feed with humic acid in direct contact membrane distillation, *Sep. Purif. Technol.* 210 (2019) 20–28.
- [170] R. Zheng, Y. Chen, J. Wang, J. Song, X.-M. Li, T. He, Preparation of omniphobic PVDF membrane with hierarchical structure for treating saline oily wastewater using direct contact membrane distillation, *J. Membr. Sci.* 555 (2018) 197–205.
- [171] N. Hamzah, C.P. Leo, Membrane distillation of saline with phenolic compound using superhydrophobic PVDF membrane incorporated with TiO₂ nanoparticles: separation, fouling and self-cleaning evaluation, *Desalination* 418 (2017) 79–88.
- [172] J. Lee, C. Boo, W.-H. Ryu, A.D. Taylor, M. Elimelech, Development of omniphobic desalination membranes using a charged electrospun nanofiber scaffold, *ACS Appl. Mater. Interfaces* 8 (2016) 11154–11161.
- [173] A.A. Khan, M.I. Siyal, J.-O. Kim, Fluorinated silica-modified anti-oil-fouling omniphobic F-SiO₂@PES robust membrane for multiple foulants feed in membrane distillation, *Chemosphere* 263 (2021), 128140.
- [174] Z.-Q. Dong, X.-H. Ma, Z.-L. Xu, Z.-Y. Gu, Superhydrophobic modification of PVDF-SiO₂ electrospun nanofiber membranes for vacuum membrane distillation, *RSC Adv.* 5 (2015) 67962–67970.
- [175] Y.-X. Huang, Z. Wang, J. Jin, S. Lin, Novel Janus membrane for membrane distillation with simultaneous fouling and wetting resistance, *Environ. Sci. Technol.* 51 (2017) 13304–13310.
- [176] M. Wen, M. Chen, G.-K. Ren, P.-L. Li, C. Lv, Y. Yao, Y.-K. Liu, S.-J. Deng, Z. Zheng, C.-G. Xu, D.-L. Luo, Enhancing the selectivity of hydrogen isotopic water in membrane distillation by using graphene oxide, *J. Membr. Sci.* 610 (2020), 118237.
- [177] K.-Y. He, Q. Wei, Y.-L. Wang, S. Wang, S.-P. Cui, Q.-Y. Li, Z.-R. Nie, Hydrophobic mesoporous organosilica membranes: preparation and application in the separation of volatile organic compounds from water, *Microporous Mesoporous Mater.* 288 (2019), 109606.
- [178] S.J. Moon, S.M. Jeon, J.H. Kim, Y.M. Lee, Membrane distillation & pressure retarded osmosis hybrid system using thermally rearranged nanofibrous membranes, *J. Membr. Sci.* 638 (2021), 119735.
- [179] L. Liu, F. Shen, X. Chen, J. Luo, Y. Su, H. Wu, Y. Wan, A novel plasma-induced surface hydrophobization strategy for membrane distillation: etching, dipping and grafting, *J. Membr. Sci.* 499 (2016) 544–554.
- [180] S. Xue, X. Xu, L. Zhang, Fabrication of ecofriendly recycled Marimo-like hierarchical micronanostructure superhydrophobic materials for effective and selective separation of oily pollutants from water, *Ind. Eng. Chem. Res.* 58 (2019) 5613–5621.
- [181] B. Zhu, W. Jiang, W. Wang, Y. Lin, T. Ruan, G. Jiang, Occurrence and degradation potential of fluoroalkylsilane substances as precursors of perfluoroalkyl carboxylic acids, *Environ. Sci. Technol.* 53 (2019) 4823–4831.
- [182] I. Sas, R.E. Gorga, J.A. Joines, K.A. Thoney, Literature review on superhydrophobic self-cleaning surfaces produced by electrospinning, *J. Polym. Sci. B Polym. Phys.* 50 (2012) 824–845.
- [183] C. Su, Y. Li, Y. Dai, F. Gao, K. Tang, H. Cao, Fabrication of three-dimensional superhydrophobic membranes with high porosity via simultaneous electrospinning and electrospinning, *Mater. Lett.* 170 (2016) 67–71.
- [184] H. Attia, D.J. Johnson, C.J. Wright, N. Hilal, Robust superhydrophobic electrospun membrane fabricated by combination of electrospinning and electrospinning techniques for air gap membrane distillation, *Desalination* 446 (2018) 70–82.
- [185] Y.C. Woo, L.D. Tijing, W.-G. Shim, J.-S. Choi, S.-H. Kim, T. He, E. Drioli, H. K. Shon, Water desalination using graphene-enhanced electrospun nanofiber membrane via air gap membrane distillation, *J. Membr. Sci.* 520 (2016) 99–110.
- [186] T. Ni, Y. You, Z. Xie, L. Kong, B. Newman, L. Henderson, S. Zhao, Waste-derived carbon fiber membrane with hierarchical structures for enhanced oil-in-water emulsion separation: Performance and mechanisms, *J. Membr. Sci.* 653 (2022), 120543.
- [187] M.K. Sarkar, K. Bal, F. He, J. Fan, Design of an outstanding super-hydrophobic surface by electro-spinning, *Appl. Surf. Sci.* 257 (2011) 7003–7009.
- [188] Y. Wang, G. He, Y. Shao, D. Zhang, X. Ruan, W. Xiao, X. Li, X. Wu, X. Jiang, Enhanced performance of superhydrophobic polypropylene membrane with modified antifouling surface for high salinity water treatment, *Sep. Purif. Technol.* 214 (2019) 11–20.
- [189] X. Li, W. Qing, Y. Wu, S. Shao, L.E. Peng, Y. Yang, P. Wang, F. Liu, C.Y. Tang, Omniphobic nanofibrous membrane with pine-needle-like hierarchical nanostructures: toward enhanced performance for membrane distillation, *ACS Appl. Mater. Interfaces* 11 (2019) 47963–47971.
- [190] S. Zhao, Z. Tao, M. Han, Y.-x. Huang, B. Zhao, L. Wang, X. Tian, F. Meng, Hierarchical Janus membrane with superior fouling and wetting resistance for efficient water recovery from challenging wastewater via membrane distillation, *J. Membr. Sci.* 618 (2021), 118676.
- [191] S. Amigoni, E. Taffin de Givenchy, M. Dufay, F. Guittard, Covalent layer-by-layer assembled superhydrophobic organic-inorganic hybrid films, *Langmuir* 25 (2009) 11073–11077.
- [192] C.W. Extrand, Model for contact angles and hysteresis on rough and ultraphobic surfaces, *Langmuir* 18 (2002) 7991–7999.
- [193] X. Chen, J.A. Weibel, S.V. Garimella, Water and ethanol droplet wetting transition during evaporation on omniphobic surfaces, *Sci. Rep.* 5 (2015) 1–11.
- [194] J. Barman, S.K. Majumder, P.K. Roy, K. Khare, Tunable superoleophobicity via harnessing the surface chemistry of UV responsive titania coatings, *RSC Adv.* 8 (2018) 13253–13258.
- [195] A. Grigoryev, I. Tokarev, K.G. Kornev, I. Luzinov, S. Minko, Superomniphobic magnetic microtextures with remote wetting control, *J. Am. Chem. Soc.* 134 (2012) 12916–12919.
- [196] X. Tian, V. Jokinen, J. Li, J. Sainio, R.H. Ras, Unusual dual superlyophobic surfaces in oil-water systems: the design principles, *Adv. Mater.* 28 (2016) 10652–10658.

- [197] J. Dong, J. Zhang, Biomimetic super anti-wetting coatings from natural materials: superamphiphobic coatings based on nanoclays, *Sci. Rep.* 8 (2018) 1–12.
- [198] A.K. Kota, W. Choi, A. Tuteja, Superomniphobic surfaces: design and durability, *MRS Bull.* 38 (2013) 383–390.
- [199] Z. Han, B. Tay, C. Tan, M. Shakerzadeh, K. Ostrikov, Electrowetting control of Cassie-to-Wenzel transitions in superhydrophobic carbon nanotube-based nanocomposites, *ACS Nano* 3 (2009) 3031–3036.
- [200] A. Grigoryev, Y. Roiter, I. Tokarev, I. Luzinov, S. Minko, Colloidal occlusion template method for micromanufacturing of omniphobic surfaces, *Adv. Funct. Mater.* 23 (2013) 870–877.
- [201] A. Ahuja, J. Taylor, V. Lifton, A. Sidorenko, T. Salamon, E. Lobaton, P. Kolodner, T. Krupenkin, Nanonails: a simple geometrical approach to electrically tunable superlyophobic surfaces, *Langmuir* 24 (2008) 9–14.
- [202] M. Im, H. Im, J.-H. Lee, J.-B. Yoon, Y.-K. Choi, A robust superhydrophobic and superoleophobic surface with inverse-trapezoidal microstructures on a large transparent flexible substrate, *Soft Matter* 6 (2010) 1401–1404.
- [203] K. Ellinas, A. Tserepi, E. Gogolides, From superamphiphobic to amphiphilic polymeric surfaces with ordered hierarchical roughness fabricated with colloidal lithography and plasma nanotexturing, *Langmuir* 27 (2011) 3960–3969.
- [204] R. Castro-Munoz, Breakthroughs on tailoring pervaporation membranes for water desalination: a review, *Water Res.* 187 (2020), 116428.
- [205] A. Tuteja, W. Choi, G.H. McKinley, R.E. Cohen, M.F. Rubner, Design parameters for superhydrophobicity and superoleophobicity, *MRS Bull.* 33 (2008) 752–758.
- [206] K.J. Lu, J. Zuo, J. Chang, H.N. Kuan, T.-S. Chung, Omniphobic hollow-fiber membranes for vacuum membrane distillation, *Environ. Sci. Technol.* 52 (2018) 4472–4480.
- [207] T.G. Ambaye, M. Vaccari, S. Prasad, S. Rtimi, Recent progress and challenges on the removal of per- and poly-fluoroalkyl substances (PFAS) from contaminated soil and water, *Environ. Sci. Pollut. Res.* 29 (2022) 58405–58428.
- [208] M. Li, F. Sun, W. Shang, X. Zhang, W. Dong, Z. Dong, S. Zhao, Removal mechanisms of perfluorinated compounds (PFCs) by nanofiltration: roles of membrane-contaminant interactions, *Chem. Eng. J.* 406 (2021), 126814.
- [209] S.S. Ray, C.K. Deb, H.M. Chang, S.S. Chen, M. Ganesapillai, Crosslinked PVDF-HFP-based hydrophobic membranes incorporated with CNF for enhanced stability and permeability in membrane distillation, *J. Appl. Polym. Sci.* 136 (2019) 48021.
- [210] W.-T. Xu, Z.-P. Zhao, M. Liu, K.-C. Chen, Morphological and hydrophobic modifications of PVDF flat membrane with silane coupling agent grafting via plasma flow for VMD of ethanol–water mixture, *J. Membr. Sci.* 491 (2015) 110–120.
- [211] N. Hamzah, M. Nagarajah, C. Leo, Membrane distillation of saline and oily water using nearly superhydrophobic PVDF membrane incorporated with SiO₂ nanoparticles, *Water Sci. Technol.* 78 (2018) 2532–2541.
- [212] F. Ardeshiri, S. Salehi, M. Peyravi, M. Jahanshahi, A. Amiri, A.S. Rad, PVDF membrane assisted by modified hydrophobic ZnO nanoparticle for membrane distillation, *Asia Pac. J. Chem. Eng.* 13 (2018), e2196.
- [213] S. Leaper, A. Abdel-Karim, B. Faki, J.M. Luque-Alled, M. Alberto, A. Vijayaraghavan, S.M. Holmes, G. Szekely, M.I. Badawy, N. Shokri, Flux-enhanced PVDF mixed matrix membranes incorporating APTS-functionalized graphene oxide for membrane distillation, *J. Membr. Sci.* 554 (2018) 309–323.
- [214] M.S. Salem, A.H. El-Shazly, N. Nady, M.R. Elmarghany, M.N. Sabry, PES/PVDF blend membrane and its composite with graphene nanoplates: preparation, characterization, and water desalination via membrane distillation, *Desalin. Water Treat.* 166 (2019) 9–23.
- [215] L. Dumée, V. Germain, K. Sears, J. Schütz, N. Finn, M. Duke, S. Cerneaux, D. Cornu, S. Gray, Enhanced durability and hydrophobicity of carbon nanotube bucky paper membranes in membrane distillation, *J. Membr. Sci.* 376 (2011) 241–246.
- [216] L.F. Dumée, K. Sears, J. Schütz, N. Finn, C. Huynh, S. Hawkins, M. Duke, S. Gray, Characterization and evaluation of carbon nanotube Bucky-Paper membranes for direct contact membrane distillation, *J. Membr. Sci.* 351 (2010) 36–43.
- [217] I.V. Korolkov, Y.G. Gorin, A.B. Yeszhanov, A.L. Kozlovskiy, M.V. Zdorovets, Preparation of PET track-etched membranes for membrane distillation by photo-induced graft polymerization, *Mater. Chem. Phys.* 205 (2018) 55–63.
- [218] D. Hou, K.S. Christie, K. Wang, M. Tang, D. Wang, J. Wang, Biomimetic superhydrophobic membrane for membrane distillation with robust wetting and fouling resistance, *J. Membr. Sci.* 599 (2020), 117708.
- [219] S.S. Hussein, S.S. Ibrahim, M.A. Toma, Q.F. Alsalhy, E. Drioli, Novel chemical modification of polyvinyl chloride membrane by free radical graft copolymerization for direct contact membrane distillation (DCMD) application, *J. Membr. Sci.* 611 (2020) 118266.
- [220] M. Khatri, L. Francis, N. Hilal, Modified electrospun membranes using different nanomaterials for membrane distillation, *Membranes* 13 (2023) 338.
- [221] L. Zhao, C. Wu, X. Lu, D. Ng, Y.B. Truong, Z. Xie, Activated carbon enhanced hydrophobic/hydrophilic dual-layer nanofiber composite membranes for high-performance direct contact membrane distillation, *Desalination* 446 (2018) 59–69.
- [222] T. Chen, A. Soroush, M.S. Rahaman, Highly hydrophobic electrospun reduced graphene oxide/poly (vinylidene fluoride-co-hexafluoropropylene) membranes for use in membrane distillation, *Ind. Eng. Chem. Res.* 57 (2018) 14535–14543.
- [223] L.F. Dumée, S. Gray, M. Duke, K. Sears, J. Schütz, N. Finn, The role of membrane surface energy on direct contact membrane distillation performance, *Desalination* 323 (2013) 22–30.
- [224] J. Ren, J. Li, Z. Xu, Y. Liu, F. Cheng, Simultaneous anti-fouling and flux-enhanced membrane distillation via incorporating graphene oxide on PTFE membrane for coking wastewater treatment, *Appl. Surf. Sci.* 531 (2020), 147349.
- [225] N. Sun, J. Li, J. Ren, Z. Xu, H. Sun, Z. Du, H. Zhao, R. Ettelatie, F. Cheng, Insights into the enhanced flux of graphene oxide composite membrane in direct contact membrane distillation: the different role at evaporation and condensation interfaces, *Water Res.* 212 (2022), 118091.
- [226] I.V. Korolkov, A.B. Yeszhanov, M.V. Zdorovets, Y.G. Gorin, O. Güven, S. S. Dosmagambetova, N.A. Khlebnikov, K.V. Serkov, M.V. Krasnopyorova, O. S. Milts, Modification of PET ion track membranes for membrane distillation of low-level liquid radioactive wastes and salt solutions, *Sep. Purif. Technol.* 227 (2019), 115694.
- [227] W. Qing, Y. Wu, X. Li, X. Shi, S. Shao, Y. Mei, W. Zhang, C.Y. Tang, Omniphobic PVDF nanofibrous membrane for superior anti-wetting performance in direct contact membrane distillation, *J. Membr. Sci.* 608 (2020), 118226.